

An-Najah National University

Faculty of Graduate Studies

**Modification and Characterization of Novel Porous SiO₂
Material Functionalized with C,C-Pyridylpyrazole acceptor
for sulphate Removal from wastewater**

By

Deena Adnan Ali Khudariah

Supervisor

Prof. Shehdeh Jodeh

Co-Supervisor

Prof. Ismail Warad

**This Thesis is Submitted in Partial Fulfillment of the Requirements for
The Degree of Master of Chemistry, Faculty of Graduate Studies,
An-Najah National University, Nablus - Palestine.**

2016

**Modification and Characterization of Novel Porous
SiO₂ Material Functionalized with C,C-
Pyridylpyrazole acceptor for sulphate Removal from
waste water**

by

Deena Adnan Ali Khudariah

This Thesis was defended successfully on 1 /11/2016 and approved by:

Defense Committee Members

Signature

- Prof. Shehdeh Jodeh / Supervisor

Shehdeh Jodeh

- Prof. Ismail Warad / Co-Supervisor

Ismail Warad

- Dr. Sobhi Samhan / External Examiner

Sobhi Samhan

- Dr. Nidal Zater / Internal Examiner

Nidal Zater

Dedication

I dedicate this thesis to my beloved father and mother

They have successfully made me the person I am becoming

And

To my uncle

Dr. Adel Khudariah

For being great pillar of support

I also dedicate this work to my husband and my children

Acknowledgements

First of all, praise be to Allah for helping me in making this thesis possible. I would like to express my sincere gratitude to prof. Shehdeh Joudeh for his supervision, guidance and constructive advice. Our thanks also go to prof. Ismail Warad.

Thanks go also to Middle East Desalination Research Center (MEDRC) who funded my project through the Palestinian water authority whom our thanks go as well to them for their follow up the project.

My parents, my husband and my uncle, thank you for being a great source of support and encouragement. I am grateful to all of you for your love, moral support, and patience. All my friends and fellow graduate students, thank you.

الإقرار

أنا الموقع أدناه مقدم الرسالة التي تحمل العنوان:

**Modification and Characterization of Novel Porous SiO₂ Material
Functionalized with C,C-Pyridylpyrazole acceptor for sulphate
Removal from waste water**

أقر بأن ما اشتملت عليه هذه الرسالة إنما هي نتاج جهدي الخاص, باستثناء ما تمت الإشارة إليه
حيثما ورد, وأن هذه الرسالة ككل, أو أي جزء منها لم يُقدم لنيل أية درجة أو لقب علمي أو بحثي
لدى أي مؤسسة تعليمية أو بحثية أخرى.

Declaration

The work provided in this thesis, unless otherwise referenced, is the
researcher's own work, and has not been submitted elsewhere for any other
degree or qualification.

Student's name: Deena Adnan Ali Khudariah

اسم الطالب:

Signature:

د. دينا

التوقيع:

Date:

2016/11/1

التاريخ:

Table of contents

No.	Content	Page
	Dedication	III
	Acknowledgement	IV
	Declaration	V
	Table of contents	VI
	List of tables	IX
	List of figures	X
	List of abbreviations	XII
	Abstract	XIV
	Chapter One: Introduction	1
1.1	Overview	1
1.2	Objective	4
1.2.1	General objectives	4
1.2.2	Specific objectives	4
1.3	Research questions and identified problems	4
1.4	Significance of thesis	5
1.5	Novelty of the work	5
	Chapter Two: Background and Literature review	6
2.1	Water resources in Palestine	6
2.1.1	Ground water	7
2.1.2	Ground water contamination	13
2.1.3	Sources of ground water pollution	14
2.2	Sulfate	16
2.2.1	Occurrence	17
2.3	Adsorption	20
2.3.1	Adsorption in liquids	21
2.3.2	Adsorption in solids	22

2.3.3	Types of adsorption	22
2.3.4	Adsorption Isotherm Models	24
2.3.4.1	Langmuir Adsorption Isotherm	25
2.3.4.2	Freundlich model Isotherm	26
2.3.4.3	Temkin model Isotherm	27
2.3.5	Thermodynamics studies	27
2.3.6	Adsorption kinetics	28
2.3.6.1	Pseudo-First-Order equation	28
2.3.6.2	Pseudo-Second-Order equation	29
2.4	Polysiloxane	29
2.4.1	Functionalized Polysiloxane surfaces	30
2.4.2	Polysiloxane surface modified with a functional C,C-Pyridylpyrazole ligand	30
	Chapter Three: Experimental Work	32
3.1	Chemical Materials	32
3.2	Instrumentations	33
3.3	Methodology	33
3.4	Immobilization of C,C-Pyridylpyrazole compound on silica gel surface	34
3.5	Preparation of sulfate solutions	34
3.6	Calibration Curve	34
3.7	Determination of sulfate-ion contamination	35
3.8	Batch Experiment	36
3.8.1	Effect of contact time	36
3.8.2	effect of temperature	36
3.8.3	effect of pH	37
3.8.4	effect of Adsorbent dose	37
3.8.5	effect of initial concentration of sulfate	37
	Chapter Four: Results and Discussion	38
4.1	Characterization of Materials	38

4.1.1	SEM Characterization	38
4.1.2	IR Characterization of the material	39
4.1.3	Thermogravimetric Analysis	40
4.2	Investigation of adsorption parameters	41
4.2.1	Effect of contact time on sulfate adsorption	41
4.2.2	Temperature effect on sulfate adsorption	42
4.2.3	Effect of pH on sulfate adsorption	43
4.2.4	The Effect of adsorbent dose	44
4.2.5	Effect of sulfate concentration	45
4.3	Adsorption isotherm of sulfate	48
4.3.1	Langmuir Adsorption Isotherm	48
4.3.2	Freundlich Adsorption Isotherm	50
4.3.3	Temkin Adsorption Isotherm	51
4.4	Adsorption Thermodynamics	53
4.5	Adsorption Kinetics of sulfate	54
	Conclusions	56
	Recommendations	56
	References	57
	الملخص	ب

List of Tables

No.	Table	Page
4.1	Adsorption parameter	48
Table 4.2	Parameters and correlation coefficient of Langmuir isotherm model for adsorption of sulfate onto (Si-C ₃ H ₆ NPyrPz)	49
Table 4.3	Parameters and correlation coefficient of Freundlich isotherm model for adsorption of sulfate onto (Si-C ₃ H ₆ NPyrPz)	51
Table 4.4	Temkin isotherm model parameters and correlation coefficient for adsorption of sulfate on(Si-C ₃ H ₆ NPyrPz)	52
Table 4.5	The values of the thermodynamic of sulfate adsorption at various temperatures.	53
Table 4.6	Pseudo first order kinetic model parameters for sulfate adsorption onto (Si-C ₃ H ₆ NPyrPz) at 20°C.	54
Table 4.7	Pseudo second order model parameters for sulfate adsorption onto (Si-C ₃ H ₆ NPyrPz) at 20°C.	55

List of Figures

No.	Figure	Page
Figure 2.1	Groundwater aquifer in mandate Palestine	11
Figure 2.2	The distribution of groundwater well in mandate Palestine	12
Figure 2.3	Sulfate concentration in the groundwater of the Gaza Strip 2008	20
Figure 2.4	Adsorption in liquids	21
Figure 2.5	Adsorption in solids	22
Figure 2.6	Physical Adsorption vs. Temperature	23
Figure 2.7	Chemical Adsorption vs. Temperature	24
Figure 3.1	The synthesis procedure of (Si-RO-PzPyr)	33
Figure 3.2	Linear calibration curve of absorbance vs. concentration for sulfate	35
Figure 4.1	SEM images of Free Silica and synthesized Polysiloxane surface (Si-RO-PzPyr)	38
Figure 4.2	IR spectra of pure silica and modified silica	39
Figure 4.3	Thermogravimetric curves of free silica, epoxy silica (Si-Ep) and modified silica (Si-RO-PzPyr)	41
Figure 4.4	Effect of contact time to determine the time of maximum adsorption of sulfate. (Temp.= 25°C, pH= 3.7, Conc. Of sulfate = 20mg/L, sol. Volume= 50 mL, adsorbent dose= 0.005 g)	42
Figure 4.5	Effect of temperature on sulfate adsorption. (c_o = 20 ppm, time= 30 min., adsorbent dose= 0.005 g, sol. Volume= 50 mL)	43
Figure 4.6	pH effect on sulfate adsorption. (C_o = 20 ppm, time= 30 min., T=30°C, adsorbent dose= 0.005 g, sol. Volume= 50 mL)	43
Figure 4.7	Effect of dosage of adsorbent on the removal of sulfate. (Temp.= 30°C, time= 30 min., pH= 2, conc. of sulfate= 20 mg/L, sol. Volume= 50 mL)	44
Figure 4.8	Effect of sulfate Conc. on adsorption(temp.= 30°CpH= 2, time =30 min., adsorbent dose= 15mg)	45

Figure 4.9	Effect of sulfate concentration on adsorption capacity. (temp.= 30°C, time =20 min., adsorbent dose= 15mg)	46
Figure 4.10	Effect of sulfate conc. On the Distribution Ratio (K_d). (Temp.= 30°C, pH= 2, sol. volume= 50 mL, adsorbent dose= 0.0015 g)	47
Figure 4.11	Langmuir plot for sulfate adsorption on (Si-RO-PzPyr). (Temp.= 30°C, pH= 2, time= 30 min., sol. Volume= 50 mL, adsorbent dose= 0.015 g)	49
Figure 4.12	Freundlich plot for sulfate adsorption on(Si-RO-PzPyr). (Temp.= 30°C, pH= 2, time= 30min., sol. Volume= 50 mL, adsorbent dose= 0.015 g)	50
Figure 4.13	Temkin plot for sulfate adsorption on (Si-RO-PzPyr). (Temp.= 30°C, pH=2, time= 30 min., sol. Volume= 50 mL, adsorbent dose= 0.015 g)	51
Figure 4.14	A graph of $\ln K_d$ vs. $1/T$ for sulfate adsorption on (Si-RO-PzPyr). pH=2, time= 30 min., sol. Volume= 50 mL, adsorbent dose= 0.005 g)	53
Figure 4.15	Pseudo-first order plot of sulfate adsorption	54
Figure 4.16	Pseudo-second order plot of sulfate adsorption	55

List of Abbreviation

Symbol	Abbreviation
A	the Temkin isotherm constant (L/g)
\AA	Angstrom = 1.0×10^{-10} meters
A_o	absorbance of methylene blue in the sample solution before treatment
Abs.	Absorbance
A_e	Absorbance of methylene blue in the sample solution after treatment
B	Dimensionless Temkin constant
B.J.H	Barrett-Joyner-Halenda method
b	Temkin constant related to heat of sorption (J/mol)
C_o	Concentration of sulfate in the sample solution before treatment (mg/L)
C_e	Concentration of sulfate in the sample solution after treatment (mg/L) at equilibrium
C_i	Initial concentration of sulfate in the sample solution (mg/L)
IQ	Intelligence Quotient
IR	Infra-Red
JSI	Jordanian Standards Institution
K_1	The Lagergren's first order rate constant
K_2	The pseudo second order rate constant
K_d	The distribution coefficient
K_F	Freundlich constant which is an approximate indicator of adsorption capacity of the sorbent (mg/g (L/mg) ^{1/n})
K_L	Langmuir isotherm constant (L/mg)
m_{sed}	Mass of adsorbent dose
n	Dimensionless Freundlich constant giving an indication of how favorable the adsorption process
PSI	Palestinian Standards Institution
Q_e	The amount of sulfate adsorbed per gram of the adsorbent (mg/g)
Q_m	Maximum monolayer coverage capacity (mg/g)
Q_t	Amount of adsorbate per unit mass of adsorbent at

	time t (min)
R	The gas constant (8.314 J/mol K)
R^2	Correlation coefficient (regression coefficient)
R_L	Dimensionless constant separation factor
SEM	Scanning Electron Microscope
Si-Ep	Activated silica gel with 3-glycidoxypropyltrimethoxysilane (epoxy-silica)
(Si-RO-PzPyr)	SiO ₂ Material Functionalized with C,C- Pyridylpyrazole Receptor
SPE	Solid Phase Extraction
t	Time
T	The absolute temperature (°K)
TGA	Thermal Gravimetric Analysis
UV	Ultra Violet
V_w	Volume of solution
WHO	World Health Organization
ΔG°	Standard free Gibbs energy
ΔH°	Standard enthalpy
ΔS°	Standard entropy
MS	The Surface Modification
S	Sulfer
hrs	Hours
min	Minute
Conc.	Concentration
Temp	Temperature
FS	Free Silica

**Modification and Characterization of Novel Porous SiO₂ Material
Functionalized with C,C-Pyridylpyrazole acceptor for sulphate
Removal from waste water**

By

Deena Adnan Ali Khudariah

Supervisor

Prof. Shehdeh Jodeh

Co-Supervisor

Prof. Ismail Warad

Abstract

Different pollutant reach every day to the ground water which is the main source of water to the Palestinian, one of these pollutants is sulfate; high sulfate concentration can unbalance the natural sulfate cycle and cause different health problem to both human beings and animals.

This research involve the modification of pure porous polysiloxane SiO₂ by condensing a functionalized C,C-pyridylpyrazole with a 3-glycidoxy-propyltrimethoxy-silane silylant agent, previously anchored on silica surface is reported. The epoxide group was opened yielding a receptor pendant group bonded to the inorganic surface. The Surface Modification (MS) was characterized by elemental analysis, infrared spectra, and SEM. This porous material exhibits good chemical and thermal stability determined by thermogravimetry curves and hence they can be used as perfect adsorbents to uptake sulfate from water. The concentration of adsorbate in the filtrate was determined using uv-spectrophotometry.

In order to investigate the adsorption efficiency for the adsorption of sulfate onto (Si-RO-PzPyr) the effect of solution condition on each adsorption process were studied. The result showed that the product have high adsorption efficiency.

These conditions that affect adsorption of sulfate were studied involve the effect of contact time, pH, temperature, adsorbent dose and the initial concentration of adsorbate. It was observed that the percentage removal of sulfate decreased with an increased initial concentration and pH while it increased with increase in solution contact time and adsorbent dose and temperature. The best equilibrium isotherm model for the adsorption process was investigated according to the value of the correlation coefficient of Langmuir and Freundlich and Temkin isotherm adsorption model. The result showed that the adsorption followed Temkin adsorption isotherm.

Also the kinetic of adsorption were investigated using pseudo first-order and pseudo second-order kinetics model. The results showed that the mechanism of these reaction followed pseudo –second order kinetic adsorption model.

In addition, Van't Hoff plot for adsorption in order to determine the values of enthalpy change and entropy change, and hence determining if the adsorption process is spontaneous or not, and if it is exothermic or endothermic one, the thermodynamic parameter of all the adsorption

proved that these process are endothermic ($\Delta H > 0$) and spontaneous ($\Delta S_0 > 0$).

Chapter One

Introduction

1.1. Overview

Different pollutants from industries such as smoke and chemicals are released into our environment without being treated causing environmental degradation affecting resources such as air, water and soil resulting in the destruction of our ecosystem and the extinction of wildlife. The main source of untreated pollution reaching every day to soil and ground water is municipal sewage.

Sulfate (SO_4^{2-}) can be found in almost all natural water. The origin of most sulfate compounds is the oxidation of sulfide ores, the presence of shale, or the industrial wastes. Sulfate is one of the major dissolved components of rain. High concentrations of sulfate in the water we drink can have a laxative effect when combined with calcium and magnesium, the two most common constituents of hardness [1]. Bacteria, which attack and reduce sulfates, form hydrogen sulfide gas (H_2S) [2].

The Environmental Protection Agency (EPA) standards for drinking water fall into two categories: Primary Standards and Secondary Standards. Primary Standards are based on health considerations and are designed to protect people from three classes of toxic pollutants -- pathogens, radioactive elements and toxic chemicals. Secondary Standards are based on taste, odor, color, corrosivity, foaming and staining properties of water. Sulfate is classified under the secondary maximum

contaminant level (SMCL) standards. The SMCL for sulfate in drinking water is 250 milligrams per liter (mg/l), sometimes expressed as 250 parts per million (ppm) [45].

How does sulphate get into water? Sulphate may be leached from the soil and is commonly found in most water supplies. Magnesium, potassium and sodium sulphate salts are all soluble in water. Calcium and barium sulphate are not very easily dissolved in water. There are several other sources of sulphate in water. Decaying plant and animal matter may release sulphate into water. Numerous chemical products including ammonium sulphate fertilizers contain sulphate in a variety of forms. The treatment of water with aluminum sulphate (alum) or copper sulphate also introduces sulphate into a water supply. Human activities such as the combustion of fossil fuels and sour gas processing release sulphur oxides to the atmosphere, some of which is converted to sulphate [3].

There are several technologies for sulfate treatment like chemical precipitation in order to sediment the sulfate as undissolved salt, evaporation, which reduce the volume of waste water with high concentration of sulfate or ion exchange and Reverse Osmosis [4].

Adsorption is a demonstrated waste water treatment that uses solid adsorbent to remove dissolved pollutants from waste water. One of the well-known adsorbents is activated carbon which is made from many carbonaceous sources including coal, coke, peat and coconut shell [5].

A new inorganic-organic polymer obtained by grafting of functionalized compound on porous silica, based on a recent synthesized C,C-bipyrazole which can act as in N,N-bidentate fashion forming thus a five member chelating ring which is part of several rings when the whole ligand is considered. The immobilization of this ligand on silica gel was carried out through a rather long arm spacer to facilitate the contact between the receiver and the metal ion. The 3-glycidoxypropyl-trimethoxysilane arm was used recently as silylating agent in the immobilization of many structures on silica gel. The modified material was used to separate and to extract sulfate from aqueous solutions. The results were compared with those obtained with the analog free organic monomer in liquid-liquid extraction with respect to capacity and selectivity. The percentages of adsorption were determined by UV-spectroscopy measurements [6].

We measured the surface area, pore volumes, and pore diameters of both porous polysiloxane and silica with nitrogen adsorption-desorption isotherms and Barrett-Joyner-Halenda (BJH) pore diameters methods [6][7].

1.2. Objectives

1.2.1. General Objectives

1. To remove sulphate from waste water, using a modified prepared material as an adsorbent for the solid-phase extraction of sulphate.
2. To specify the optimal conditions for the adsorption.

1.2.2. Specific objectives

1. To study the adsorption behaviors of the modified surface with sulphate.
2. To determine if (Si-RO-PzPyr) can be used to remove sulphate from polluted waste water.
3. To determine the extent that new silica gel compound when modified can tolerate and adsorb sulphate.
4. To specify the margin of sulphate that exists in industrial waste water in Palestine.

1.3. Research question and identified problems

The main questions addressed in this thesis are:

1. Can (Si-RO-PzPyr) be used to remove sulphate from polluted waste water?
2. The extent to which (Si-RO-PzPyr) can tolerate and adsorb sulfate?
3. What is the best dosage of (Si-RO-PzPyr) needed to adsorb the largest proportion of sulphate under the optimum conditions?
4. What is the adsorption behavior of the new surface with sulphate?

5. What is the margin of sulphate that exists in industrial waste water in Palestine?

1.4. Significance of thesis

1. Through this work we will try to discover a novel technique which is able to remove sulfate from waste water.
2. Lab scale set up to test of the method efficiency.

1.5. Novelty of the work

This research depends on modification and characterization of novel polysiloxane surfaces modified with copper receptor .The resulting adsorbent have been characterized by IR, BET surface area, ¹³C NMR solid state , SEM,UV,B.J.H. pore size, TGA and nitrogen adsorption – desorption isotherm.

The synthesized product was used to remove sulfate from water. The new modified porous silica showed good complexation properties in the presence of sulfate. The concentration of sulfate in the filtrate was determined using UV- spectroscopy.

Chapter Two

Background and Literature review

2.1. Water resources in Palestine

The main water resources available to Palestinians were groundwater, springs, and harvested rainwater [8]. There is little surface water and thus groundwater is the principal source of water in the Palestine.

Groundwater resources play a dominant role in the development of countries. Many rural and urban centers rely greatly on groundwater resources for public water supply. With the population growth and irrigation agriculture development, the water demand has significantly increased and has led to the overexploitation of groundwater. As many other countries, groundwater is almost the only reliable water resource in Palestine. It has extensively been used to meet the increasing water demand for domestic, irrigational, and industrial requirements. The aquifer system in the Palestine is highly permeable in many areas due to its geological nature. It should be kept in mind that the aquifers are easily permeable. Groundwater pollution due to point and nonpoint sources is caused mainly by agricultural practices (noticeable is the use of inorganic fertilizers (KNO_3), pesticides, and herbicides), localized industrial activities (organic pollutants and heavy metals), and inadequate or improper discharge of waste water and solid waste including hazardous materials [9][10].

The quality of drinking water is significantly dependent on the source. Fortunately, the only source of drinking water in Palestine is groundwater

which is clean and renewable. Nevertheless, people in the past looked carefully about contamination in drinking water using simple measures. Those measures were domestically altered either to filter, sediment, boil, or combine among these processes to provide a purified and a safe water source especially for infants. The responsibility for quality assurance of drinking water was transferred to the local authorities developing municipal drinking water networks. The quality of drinking water in the municipal networks is maintained by disinfection. The disinfection is the most powerful and reliable method nowadays to prevent water borne diseases [9][10].

For instance, the Palestinian standards institution (PSI) is the local authority to set the drinking water standards, which assimilates the Jordanian standards institution (JSI). Intern, the JSI relies greatly on the WHO and US EPA standards. Nonetheless, water quality issues have been neglected to a certain extent, with most attention focused on measures to solve water quantity and supply problems [10].

2.1.1. Ground water

When rain falls to the ground, the water does not stop moving. Some of it flows along the land surface to streams or lakes, some is used by plants, some evaporates and returns to the atmosphere, and some seeps into the ground. Water seeps into the ground much like a glass of water poured onto a pile of sand. As water seeps into the ground, some of it clings to particles of soil or to roots of plants just below the land surface. This moisture

provides plants with the water they need to grow. Water not used by plants moves deeper into the ground. The water moves downward through empty spaces or cracks in the soil, sand, or rocks until it reaches a layer of rock through which water cannot easily move. The water then fills the empty spaces and cracks above that layer. The top of the water in the soil, sand, or rocks is called the water table and the water that fills the empty spaces and cracks is called ground water. Water seeping down from the land surface adds to the ground water and is called recharge water. Ground water is recharged from rain water and snowmelt or from water that leaks through the bottom of some lakes and rivers. Ground water also can be recharged when water supply systems (pipelines and canals) leak and when crops are irrigated with more water than the plants can use. At least some ground water can be found almost everywhere. The water table may be deep, such as under a hillside, or shallow such as under a valley. The water table may rise or fall depending on several factors. Heavy rains or melting snow may increase recharge and cause the water table to rise. An extended period of dry weather may decrease recharge and cause the water table to fall.

What is an aquifer? Aquifer is the name given to underground soil or rock through which ground water can easily move. The amount of ground water that can flow through soil or rock depends on the size of the spaces in the soil or rock and how well the spaces are connected. The amount of spaces is the porosity. Permeability is a measure of how well the spaces are connected. Aquifers typically consist of gravel, sand, sandstone, or fractured rock such as limestone. These types of materials are permeable

because they have large connected spaces that allow water to flow through. The spaces in a gravel aquifer are called pores. The spaces in a fractured rock aquifer are called fractures. If a material contains pores that are not connected, ground water cannot move from one space to another. These materials are said to be impermeable. Materials such as clay or shale have many small pores, but the pores are not well connected. Therefore, clay or shale usually restricts the flow of ground water [11].

Groundwater is the major source of fresh water supply in the mandate Palestine. There are eleven ground water basins in mandate Palestine, of which four are located in the West Bank and Gaza Strip either partially or totally (Figure 2.1). About 1345 MCM/yr emerges from groundwater basins through more than 4000 wells (Figure 2.2). In the West Bank; the aquifer system is comprised of several rock formations from the Lower Cretaceous to the Holocene geologic age. Most of the formations are composed of carbonate rocks (mainly limestone, dolomite, chalk, marl, and clay). The aquifer system is recharged from rainfall in the West Bank. The main recharge areas are along the upper mountain slopes and ridges. The annual rainfall in the West Bank is estimated at 3407.5 MCM (PWA, 2005). Around 600-650 MCM of this rain is estimated to infiltrate the soil to replenish the aquifers annually. (Figure 2.1) also shows the distribution of groundwater basins and aquifers in the West Bank, which can be divided into three main groundwater basins, each of which can be subdivided into sub-basins. The West Bank aquifers The West Bank aquifer system is classified according to flow direction into: 1. The Western Aquifer System,

which is the largest, has a safe yield of 365 MCM per year (of which 40 MCM brackish). Eighty percent of the recharge area of this basin is located within the West Bank boundaries, whereas 80% of the storage area is located within Israeli borders. Groundwater flow is towards the coastal plain in the west, making this a shared basin between Israelis and Palestinians. The groundwater being mainly of good quality, this source is largely used for municipal supply. Israelis exploit the aquifers of this basin through 300 deep groundwater wells to the west of the Green Line, as well as through Mekorot (the Israeli water company) deep wells within the West Bank boundary. Palestinians, on the other hand, consume only about 7.5% of its safe yield. They extract their water from 138 groundwater wells tapping the Western Aquifer System (120 for irrigation and 18 for domestic use) in Qalqilya, Tulkarm, and West Nablus. There are 35 springs with an average flow discharge exceeding 0.1 L/s located in this aquifer system. 2. The Northeastern Aquifer System has an annual safe yield of 145 MCM (of which 70 MCM brackish). Palestinians consume only about 18% of the safe yield of their aquifers in the Jenin district and East Nablus (Wadi Al Far'a, Wadi El Bathan, as well as Aqrabaniya and Nassariya) for both irrigation and domestic purposes. There are 86 Palestinian wells in this aquifer system (78 irrigation wells and 8 domestic wells). The general groundwater flow is towards the Bisan natural springs in the north and northeast.

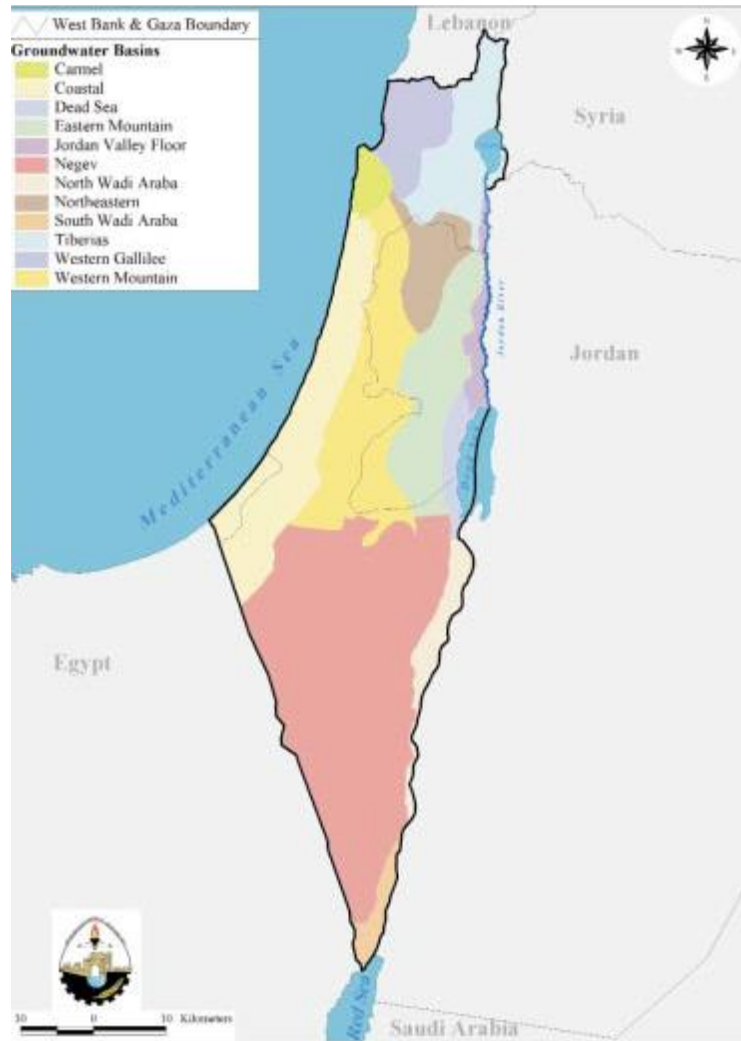


Figure 2.1. Groundwater Aquifers in mandate Palestine.



Figure 2.2. The distribution of groundwater wells in mandate Palestine.

3. The Eastern Aquifer System has a safe yield of 175 MCM per year (of which 70 MCM brackish). It lies entirely within the West Bank territory and was used exclusively by Palestinian villagers and farmers until 1967. After 1967, Israel expanded its control over this aquifer and began to tap it, mainly to supply Israeli settlements implanted in the area. The most important springs in the West Bank are in this basin. Seventy-nine springs with an average discharge greater than 0.1 L/s provide 90% of the total annual spring discharge in the West Bank. There are 122 Palestinian

groundwater wells in this aquifer system (109 for irrigation and 13 for domestic use) [46].

2.1.2. Groundwater Pollution

Any addition of undesirable substances to groundwater caused by human activities is considered to be pollution. It has often been assumed that pollutant left on or under the ground will stay there. Groundwater often spreads the effects of dumps and spills far beyond the site of the original pollution. Groundwater pollution is extremely difficult, and sometimes impossible to clean up. Groundwater pollutants come from two categories of sources: point sources and distributed, or non-point sources. Landfills, leaking gasoline storage tanks, leaking septic tanks, and accidental spills are examples of point sources. Infiltration from farm land treated with pesticides and fertilizers is an example of a non-point source [12].

Solid waste is disposed of in thousands of municipal and industrial landfills throughout the country. Chemicals that should be disposed of in hazardous waste landfills sometimes end up in municipal landfills. In addition, the disposal of many household wastes is not regulated. Once in the landfill, chemicals can leach into the ground water by means of precipitation and surface runoff. New landfills are required to have clay or synthetic liners and leachate collection systems to protect ground water. Older landfills, however, do not have these safeguards. Older landfills were often sited over aquifers or close to surface waters and in permeable soils with shallow water tables, enhancing the potential for leachate to contaminate ground

water. Closed landfills can continue to pose a ground water contamination threat if they are not capped with an impermeable material before closure to prevent the leaching of contaminants by precipitation [13].

Sewer systems are designed so that some of the sewage is degraded in the tank and some is degraded and absorbed by the surrounding sand and subsoil. Contaminants that may enter groundwater from septic systems include bacteria, viruses, detergents, and household cleaners. These can create serious pollution problems. Despite the fact that septic tanks and cesspools are known sources of contaminants, they are poorly monitored and very little studied [12][13].

2.1.3. Sources of groundwater pollution

There are many different sources of groundwater pollution. Groundwater becomes polluted when anthropogenic, or people-created, substances are dissolved or mixed in waters recharging the aquifer. Examples of this are road salt, petroleum products leaking from underground storage tanks, nitrates from the overuse of chemical fertilizers or manure on farmland, excessive applications of chemical pesticides, leaching of fluids from landfills and dumpsites, and accidental spills. Pollution also results from an overabundance of naturally occurring iron, sulphides, manganese, and substances such as arsenic. Excess iron and manganese are the most common natural contaminants. Another form of contamination results from the radioactive decay of uranium in bedrock, which creates the radioactive gas radon. Methane and other gases

sometimes cause problems. Seawater can also seep into groundwater and is a common problem in coastal areas. It is referred to as "saltwater intrusion".

These pollutants can originate from a “point source” or “non-point source” – meaning they can come from a single source (or point) or, that they don’t have one specific source and come instead from the cumulative effect of any number of factors or activities. As some of the many point- and non-point sources of groundwater pollution [12][14]:

Non-point (distributed) sources

- Fertilizers on agricultural land
- Pesticides on agricultural land and forests
- pollutants in rain, snow, and dry atmospheric fallout

Point sources

- On-site septic systems
- Leaky tanks or pipelines containing petroleum products
- Leaks or spills of industrial chemicals at manufacturing facilities
- Underground injection wells (industrial waste)
- Municipal landfills
- Livestock wastes
- Leaky sewer lines

Many natural waters and rain samples contain sulfate. Sulfate in natural waters can come from dissolved minerals, from pollutants (such as sulfuric acid), and from acid rain which has fallen or drained into the waters. Acid rain often contains Sulfates. It is usually the result of combustion of fuels which contain sulfur, primarily coal and fuel oil.

Sulfates are discharged into water from mines and smelters and from Kraft pulp and paper mills, textile mills and tanneries. Sodium, potassium and magnesium sulfates are all highly soluble in water, whereas calcium and barium sulfates and many heavy metal sulfates are less soluble. Atmospheric sulfur dioxide, formed by the combustion of fossil fuels and in metallurgical roasting processes, may contribute to the sulfate content of surface waters. Sulfur trioxide, produced by the photolytic or catalytic oxidation of sulfur dioxide, combines with water vapor to form dilute sulfuric acid, which falls as “acid rain”[15].

2.2. Sulfate

Sulphur is a non-metallic element; its common valences are -2, -1, 0, +4 and +6. The three most important sources of sulphur for commercial use are elemental sulphur, hydrogen sulphide (H_2S), found in natural gas and crude oil) and metal sulphides such as iron pyrites. Hexavalent sulphur combines with oxygen to form the divalent sulphate ion (SO_4^{2-}) [16].

Sulphates occur naturally in numerous minerals, including barite (BaSO_4), epsomite ($\text{MgSO}_4 \cdot 7\text{H}_2\text{O}$) and gypsum ($\text{CaSO}_4 \cdot 2\text{H}_2\text{O}$)[15]. The reversible

inter-conversion of sulphate and sulphide in the natural environment is known as the "sulphur cycle" [15][17].

Sulphur, principally in the form of sulphuric acid, is one of the most widely used chemicals in industrialized society. Most sulphur is converted into sulphuric acid, close to 60% of which is used for the production of phosphate and ammonium sulphate fertilizers [18].

Human activities have a major effect on the global sulfur cycle. The burning of coal, natural gas, and other fossil fuels has greatly increased the amount of S in the atmosphere and ocean and depleted the sedimentary rock sink. Sulphates or sulphuric acid products are also used in the manufacture of numerous chemicals, dyes, glass, paper, soaps, textiles, fungicides, insecticides, astringents and emetics. They are also used in the mining, pulping, metal and plating industries, in sewage treatment and in leather processing. These effluents containing Sulphates are discharged into the aquatic body. [19].

2.2.1. Occurrence

Sodium, potassium and magnesium sulphates are all soluble in water, whereas calcium and barium sulphates and the heavy metal sulphates are not. Dissolved sulphate may be reduced to sulphide, volatilized to the air as hydrogen sulphide, precipitated as an insoluble salt or incorporated in living organism [20]. Sulphates are discharged into the aquatic environment in wastes from industries that use Sulphates and sulphuric

acid, such as mining and smelting operations, Kraft pulp and paper mills, textile mills and tanneries [21]. Atmospheric sulphur dioxide (SO_2) formed by the combustion of fossil fuels and by the metallurgical roasting process, may also contribute to the sulphate content of surface waters. It has frequently been observed that the levels of sulphate in surface water correlate with the levels of sulphur dioxide in emissions from anthropogenic sources. In the Sudbury region in Ontario, for example, it was found that water quality changes such as an increase in pH and a decrease in sulphate, nickel and copper levels coincided with a reduction in sulphur dioxide emissions from the Sudbury metal smelters [22].

Sulphur trioxide (SO_3), produced by the photolytic or catalytic oxidation of sulphur dioxide, combines with water vapor to form dilute sulphuric acid, which falls as "acid" rain or snow [20].

Water Quality and Pollution Sources in Palestine, There is no database on water quality, though available data indicate that most groundwater and surface water resources are polluted by uncontrolled and untreated municipal wastewater and industrial discharge of more than 80 MCM annually. Agrochemicals also pollute water.

- Chloride levels as high as 1,000 – 1,500 milligrams per liter are found in 50 percent of Gaza domestic wells. Nitrate concentrations of up to 290 – 380 milligrams per liter have been found throughout Gaza. Both exceed WHO safe levels for drinking water of 250 mg/l for chloride and 50 mg/l for nitrates.

- Three waste water treatment plants in the West Bank and Gaza are overloaded, though only 34 percent of residents in the West Bank and 55 percent in Gaza are connected to a sewage system. Waste water is also discharged into septic tanks, cesspits, and natural water bodies.
- 75 percent of industries in Gaza and 40 percent in the West Bank are connected to sewage systems. There is little data on industrial effluents, though heavy metals and a high COD/BOD (chemical oxygen demand/biochemical oxygen demand) ratio indicate that contaminants are not biodegradable.
- Over-abstraction of groundwater for irrigation has reduced the water table and increased salinity. An annual average of 28,200 tons of fertilizer and 900 tons of pesticides (some banned by WHO such as DDT, lindanes and parathion) applied in Gaza contribute to pollution [47].

Most of the wells in Gaza have SO_4^{-2} concentrations exceeding the permissible WHO standard (Figure 2.3). The highest levels of SO_4^{-2} were in Khan Younis and the southeast, where the average concentration is 380 mg/L [48].

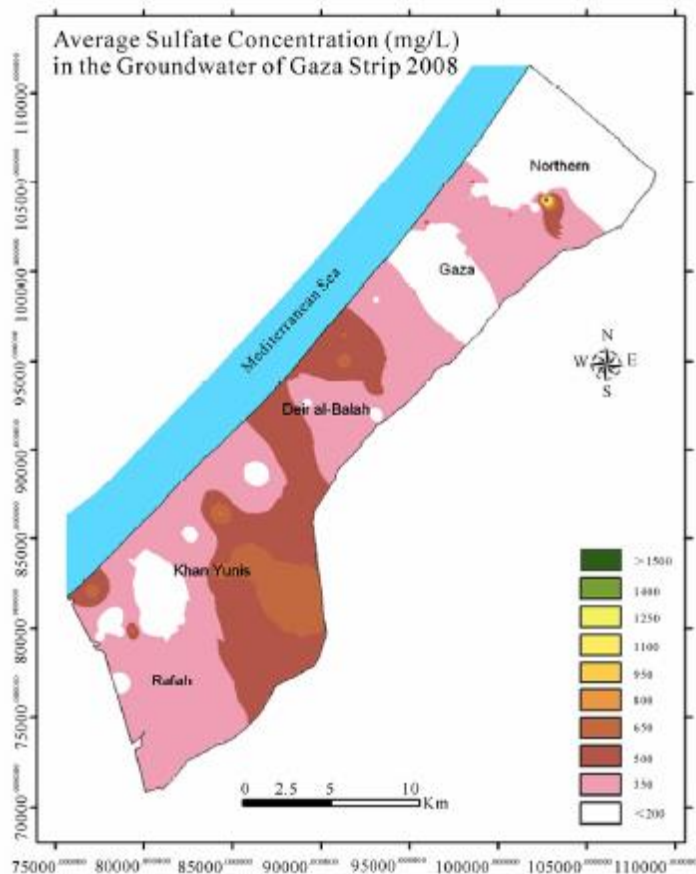


Figure 2.3. Sulfate concentrations in the groundwater of the Gaza Strip 2008.

2.3. Adsorption

Adsorption is the phenomenon of accumulation of large number of molecular species at the surface of liquid or solid phase in comparison to the bulk. The process of adsorption arises due to presence of unbalanced or residual forces at the surface of liquid or solid phase. These unbalanced residual forces have tendency to attract and retain the molecular species with which it comes in contact with the surface. Adsorption is essentially a surface phenomenon. Adsorption is a term which is completely different from Absorption .While absorption means uniform distribution of the substance throughout the bulk, adsorption essentially happens at the surface

of the substance. When both Adsorption and Absorption processes take place simultaneously, the process is called sorption. Adsorption process involves two components Adsorbent and Adsorbate. Adsorbent is the substance on the surface of which adsorption takes place. Adsorbate is the substance which is being adsorbed on the surface of adsorbent. Adsorbate gets adsorbed. Adsorbate and adsorbent give rise to adsorption [23].

2.3.1. Adsorption in liquids

Adsorption can be understood by considering a simple example. In case of liquid state, water molecule present on the surface is attracted inwards by the molecules of water present in the bulk. This gives rise to surface tension. While the molecule of water present within the bulk is equally attracted from all the sides and the net force experienced by the water molecule in bulk is zero. This clearly shows that particles at surface and particles at the bulk are in different environment. Water molecule on surface experiences unbalanced forces as compared to molecule inside which experiences forces from all direction [23].

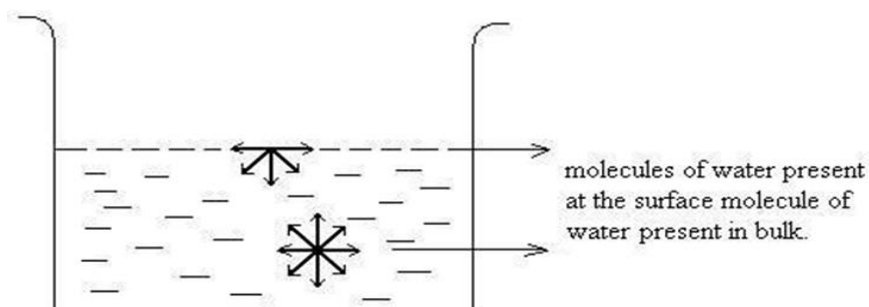


Figure 2.4. Adsorption in liquids [23].

2.3.2. Adsorption in solids

In case of solid state these residual forces arise because of unbalanced valence forces of atoms at the surface. The generation of these forces on solid surface can be explained diagrammatically as follows:

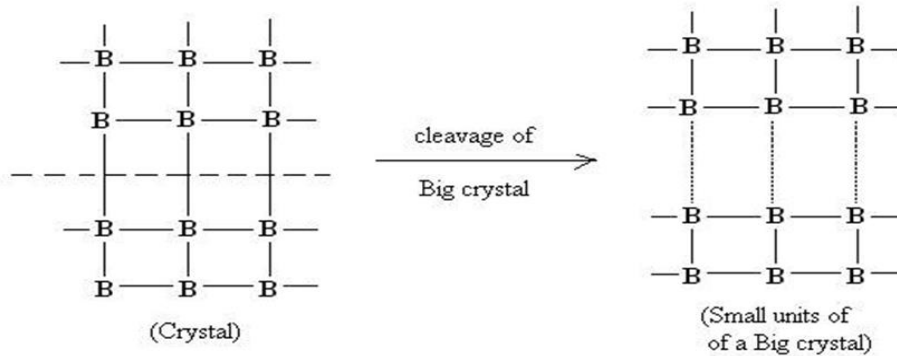


Figure 2.5. Cleavage of a big crystal into smaller unit [23].

Due to cleavage of a big crystal into smaller unit, residual forces or vacancies get generated on the surface of the solid. Occupancy of these vacancies by some other molecular species results into Adsorption [23].

2.3.3. Types of Adsorption

Forces of attraction exist between adsorbate and adsorbent. These forces of attraction can be due to Vander Waal forces of attraction which are weak forces or due to chemical bond which are strong forces of attraction. On the basis of type of forces of attraction existing between adsorbate and adsorbent, adsorption can be classified into two types: Physical Adsorption or Chemical Adsorption [23].

1. Physical Adsorption or Physisorption

When the force of attraction existing between adsorbate and adsorbent are weak Vander Waal forces of attraction, the process is called Physical Adsorption or Physisorption. Physical Adsorption takes place with formation of multilayer of adsorbate on adsorbent. It has low enthalpy of adsorption i.e. $\Delta H_{\text{adsorption}}$ is 20-40KJ/mol. It takes place at low temperature below boiling point of adsorbate. As the temperature increases in, process of Physisorption decreases [23].

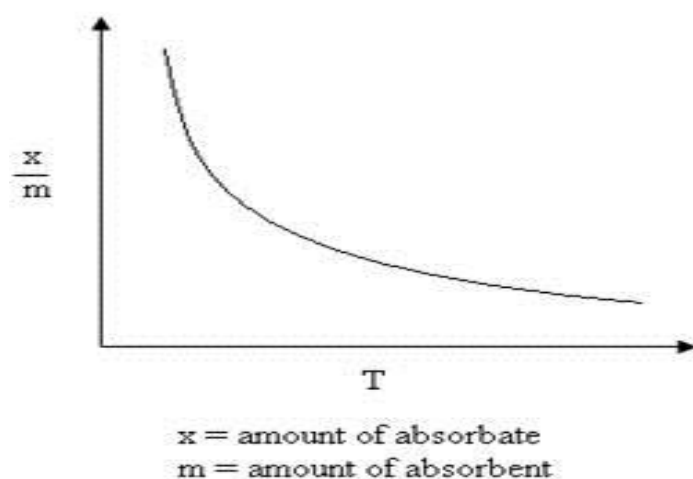
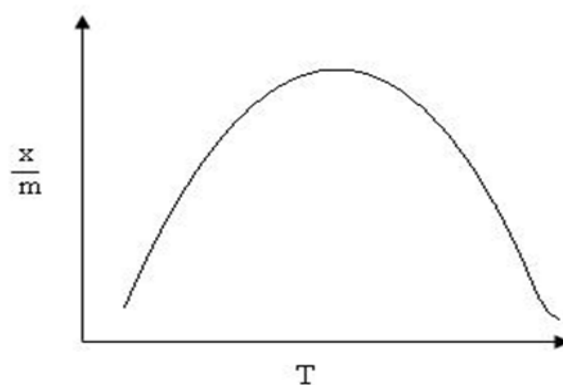


Figure 2.6. Physical Adsorption vs. Temperature [23].

2. Chemical Adsorption or Chemisorption

When the force of attraction existing between adsorbate and adsorbent are chemical forces of attraction or chemical bond, the process is called Chemical Adsorption or Chemisorption. Chemisorption takes place with formation of unilayer of adsorbate on adsorbent. It has high enthalpy of adsorption, i.e. $\Delta H_{\text{adsorption}}$ is 200-400KJ/mol.

It can take place at all temperature. With the increases in temperature, Chemisorption first increases and then decreases [23].



x = amount of adsorbate
m = amount of adsorbent

Figure 2.7. Chemical Adsorption vs. Temperature[23].

2.3.4. Adsorption isotherms models

Equilibrium study on adsorption provides information on the capacity of the adsorbent. An adsorption isotherm is characterized by certain constant values, which express the surface properties and affinity of the adsorbent and can also be used to compare the adsorptive capacities of the adsorbent for different pollutants [24].

Equilibrium data can be analyzed using commonly known adsorption systems. Several mathematical models can be used to describe experimental data of adsorption isotherms. The Freundlich, Langmuir and Temkin models are employed to analysis adsorption occurred in the experiment [25].

2.3.4.1. Langmuir Isotherm Model

In its formulation, this empirical model assumes monolayer adsorption (the adsorbed layer is one molecule in thickness), with adsorption can only occur at a finite (fixed) number of definite localized sites, that are identical and equivalent, with no lateral interaction and steric hindrance between the adsorbed molecules, even on adjacent sites. In its derivation, Langmuir isotherm refers to homogeneous adsorption, which each molecule possess constant enthalpies and sorption activation energy (all sites possess equal affinity for the adsorbate) with no transmigration of the adsorbate in the plane of the surface [26].

Based upon these assumptions, Langmuir represented the following equation [27][28]:

$$\frac{C_e}{q_e} = \frac{1}{q_m} C_e + \frac{1}{q_m K_L} \quad (2.1)$$

Where:

C_e = the concentration of the adsorbate at equilibrium (mg/L)

q_e = the amount of sulfate adsorbed per gram of adsorbent (mg/g)

q_m = Maximum capacity of monolayer coverage (mg/g)

K_L = Langmuir isotherm constant (L/mg)

The essential characteristics of the Langmuir isotherm can be expressed in terms of a dimensionless constant separation factor R_L that is given by the following equation [29]:

$$R_L = \frac{1}{(1+K_L C_o)} \quad (2.2)$$

Where C_o is the highest initial concentration of adsorbate (mg/L)

The R_L value indicates the shape of the isotherm to be either unfavorable if ($R_L > 1$), Linear if ($R_L = 1$), favorable if ($0 < R_L < 1$), or irreversible if ($R_L = 0$).

2.3.4.2. Freundlich Isotherm Model

Freundlich isotherm is the earliest known relationship describing the non-ideal and reversible adsorption, not restricted to the formation of monolayer. This empirical model can be applied to multilayer adsorption, with non-uniform distribution of adsorption heat and affinities over the heterogeneous surface. This model is defined by the following equation:

$$q_e = K_F C_e^{1/n} \rightarrow \ln q_e = \frac{1}{n} \ln C_e + \ln K_F \quad (2.3)$$

K_F and n are Freundlich constants. K_F is a rough indicator of the adsorption capacity of the sorbent and n giving an indication of the favorable way of the adsorption process. The magnitude of the exponent, $1/n$, gives an indication of the adsorption favorability [30][31].

2.3.4.3. Temkin Isotherm Model

The Temkin model is linearly represented as equation (2.4) and generally applied in the form [25][26][27]:

$$q_e = B \ln C_e + B \ln A \quad (2.4)$$

Where A and B are the Temkin isotherm constant (L/g) and heat of sorption (J/mol) respectively. R is the gas constant (J/mol/k), b is the Temkin isotherm constant linked to the energy parameter, B, as shown on the following equation:

$$b = \frac{RT}{B} \quad (2.5)$$

Where T the absolute temperature (°K)

2.3.5. Thermodynamic studies

In order to determine the thermodynamic feasibility and the thermal effects of the sorption, the Gibbs free energy (ΔG°) the entropy ΔS° and the enthalpy (ΔH°) were calculated. The ΔG° is the fundamental criterion to determine if a process occurs spontaneously. For a given temperature, a phenomenon is considered to be spontaneous if the ΔG° has a negative value. Moreover, if ΔH° is positive, the process is endothermic and if it is negative, the process is exothermic. For the determination of ΔH° and ΔS° , the relationship between sorption equilibrium constant b and Gibbs free energy was considered at any temperature [31][32].

$$\ln b = \frac{\Delta S^\circ}{R} - \frac{\Delta H^\circ}{RT} = -\frac{\Delta G^\circ}{RT} \quad (2.6)$$

The plot of $\ln b$ as a function of $1/T$ (Fig. 14) should give a linear relationship with slope of $\Delta H^\circ/R$ and an intercept of $\Delta S^\circ/R$. Then ΔG° is obtained at any temperature from the following equation [31][32]:

$$\Delta G^\circ = \Delta H^\circ - T\Delta S^\circ \quad (2.7)$$

2.3.6. Adsorption kinetics

Fitting the experimental data into different kinetic models enables to study the adsorption rate, model the process and predict information about adsorbent/adsorbate interaction (physisorption or chemisorption). Three different models can be used such as the pseudo-first-order, the pseudo-second-order and intra-particle diffusion [33].

2.3.6.1. Pseudo-First-Order Equation

Pseudo-first-order equation was given by Lagergren and Svenska (1898) to determine the rate constant of adsorption process as:

$$\log(q_e - q_t) = \log q_e - \left(\frac{K_1}{2.303}\right)t \quad (2.8)$$

Where q_e is the adsorption capacity of the adsorbent at equilibrium (mg/g), q_t is the amount of sulfate adsorbed at time t (mg/g) and K_1 is the pseudo first order rate constant (min^{-1}). Values of k_1 and q_e were calculated from the slope and the intercept of the plots of $\log(q_e - q_t)$ versus t respectively at different concentrations [34][35].

2.3.6.2. Pseudo-second-Order Equation

Equation of pseudo-second-order based on equilibrium adsorption can be expressed as:

$$\frac{t}{q_t} = \frac{1}{q_e} t + \frac{1}{K_2 q_e^2} \quad (2.9)$$

Where k_2 (g/mg•min) is the adsorption rate constant of pseudo-second-order adsorption rate. The value of q_e and k_2 can be obtained from the slope and the intercept of the plot of t/q_t versus t respectively [34][35].

2.4. Polysiloxane

Polysiloxanes, or polymerized siloxanes, are a polymer with a silicon-oxygen backbone. Its chemical formula is $(R_2SiO)_n$, where R is usually methylsiloxanes (CH_3), although it can be H or alkyl or aryl group. Polysiloxane has shown greater resistance to the effects of UV radiation than organic polymers containing a carbon-carbon backbone. Polysiloxanes can be oils, greases, rubbers or plastics depending on molecular weight. Polysiloxanes refer to a wide range of fluids, resins, or elastomers, which are made from polymerizations of siloxanes. The siloxanes consist of alternating silicon and oxygen atoms. Some useful properties of polysiloxanes such as flexibility, chemical inertness, permeability to gases, Resistance to water and oxidation, Low glass transition temperature, low surface energy [36].

2.4.1. Functionalized polysiloxane surfaces

There are two common methods used to prepare these functionalized ligand systems. The first method is the sol-gel process which involves hydrolysis and condensation of $\text{Si}(\text{OEt})_4$ with the appropriate silane coupling agent $(\text{RO})_3\text{SiX}$ where X represents an organofunctionalized ligand. The second approach is the chemical modification of the pre-prepared functionalized Polysiloxane. The second method appears as an interesting alternative mainly on account of substitution of organofunctionalized groups when appropriate chelating silane agents are difficult to prepare. The main advantages of these functionalized inorganic supports are their high thermal, hydrolytic and mechanical stability in addition to lack of swelling in solvents. These functionalized systems have been used in many important applications such as; chemisorption, recovery and separation of metal cations from organic solvents and aqueous solutions. In addition they were used widely as stationary phases in chromatography and as heterogeneous catalysts [37][38].

2.4.2. Polysiloxane modified with a functional C, C-Pyridylpyrazole ligand

In recent years, great interest has been devoted to the preparation and study of organofunctionalized silica gels due to their multiple uses in particular, in concentration and separation processes. These systems can be operated indefinitely without loss of the expensive organic molecules and maintain the selectivity shown toward metal ions in aqueous solution by the

particular ligand in the Free State. The potential applications of these systems are due essentially to the nature of the grafted ligands. Indeed, the most commonly attached chelate ability for this purpose is devoted for donor atoms, such as oxygen, nitrogen and sulphur which have a large capability in forming complexes with a series of metal ions, forcing in some cases, a distinguishable selective extraction property [39].

In this context, the ability of pyrazole and its derivatives to act as ligands with sp^2 hybrid nitrogen donors are evident from the large number of articles, several of them being reviews. In our recent works, a series of acyclic pyrazole compounds containing one, two, three or four pyrazole rings were prepared and demonstrated to extract bivalent metal cations, whereas macrocyclic pyrazolic compounds are expected to also form stable complexes with alkali metals. However, the chemistry of the pyrazole compounds bonded to silica gel has not yet been sufficiently developed [39,40].

Chapter Three

Experimental Work

3.1. Chemical Materials

Solvents and other chemicals obtained from suppliers, were of analytical standard which be used without additional refining. Silica gel with particle size of 70–230 mesh, average pore diameter 60A° [41], was activated by heating it to 160°C for 24 hrs.

The agent 3-glycidoxypropyltrimethoxysilane (≥98%) [42] was used without purification. Ethanol, Na₂SO₄, BaCl₂, HCl, NaOH, methanol, dichloromethane and acetonitrile were used for reflux extraction

3.2. Instrumentations

The required apparatus are: pH meter (model: 3510, JENWAY), centrifuge (model: 1020 DE, Centurion Scientific), Shaking Water Bath (Daihan Labtech, 20 to 250 rpm Digital Speed Control), UV-visible spectrophotometer (model: UV-1601, SHIMADZU), FT-IR Spectrometer (Nicolet iS5, iD3 ATR, Thermo Scientific), TGA Q50 V20.10 Build 36 instrument with heating rate of 50°C/min and in N₂ gaseous atmosphere, Differential Scanning Calorimeter (DSC) Q200, TA Instruments, scanning electron micrograph (SEM).

3.3. Methodology

The synthetic procedure to synthesis of the modified silica gel (Si-RO-PzPyr) which we will be used in this research can be summarized at Fig.3.1.

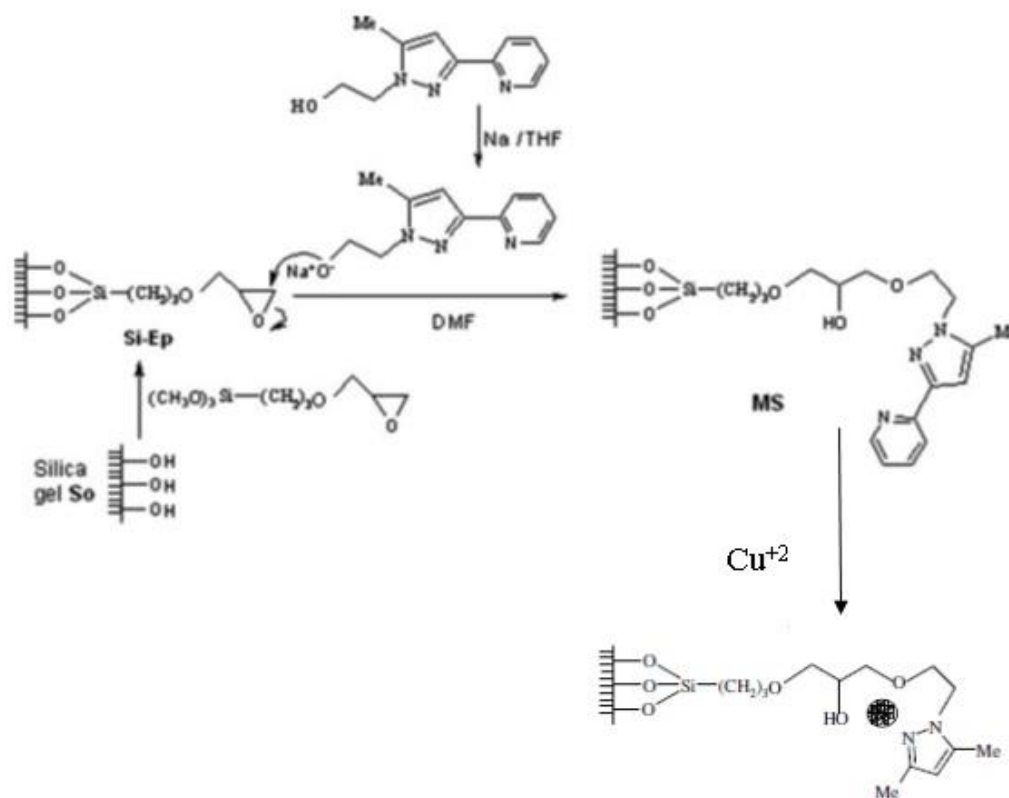


Figure 3.1: The synthesis procedure of (Si-RO-PzPyr) [7].

The first step of the synthesis consists of reacting the activated silica gel with 3-glycidoxypropyltrimethoxysilane to produce the epoxy-silica which works as antecedent for immobilizing the molecule holds the donor atom. The second step includes condensation of the C,Cpyridylpyrazole salt with epoxy silica to form the desired material MS [7].

3.4. Immobilization of C, C-pyridylpyrazole on silica gel surface

First the hydroxy-substituted C,C-pyridylpyrazole was converted into the alcoholate derivative using sodium metal in tetrahydrofuran. The produced salt was added to a suspension of epoxy-substituted silica (10 g) in 300 mL of dimethylformamide (DMF). The mixture was stirred and refluxed under nitrogen for 24 h. The produced salt was added to a suspension of epoxy-substituted silica (10 g) in 300 mL of dimethylformamide (DMF). The mixture was stirred and refluxed under nitrogen for 24 h. The mixture was filtered and the solid material was washed with 150 mL of each of DMF, toluene, distilled and deionized water, methanol, and dichloromethane and then dried [7].

3.5. Preparation of sulfate solution

A 1000 ppm concentration of stock solution of sulfate was prepared by dissolving 1.4792 g of dry Na_2SO_4 in distilled water and diluted to 1000 mL in volumetric flask.

3.6. Calibration Curve

Standard sulfate solutions of concentration 10, 20, 30, 40 and 50 mg/L were prepared by transferring 1, 2, 3, 4 and 5 mL of 1000 mg/L stock solution into 100 mL volumetric flask. Then 2 mL of 1 M HCL are added to each flask, followed by 2 mL of 25% barium chloride solution. The volume were completed to the mark with distilled water, stoppered and shaken for 1 min

by inverting several times. The absorbance of each standard was measured at 485 nm. The calibration curve was constructed by plotting absorbance versus concentration as shown in Fig. 3.2.

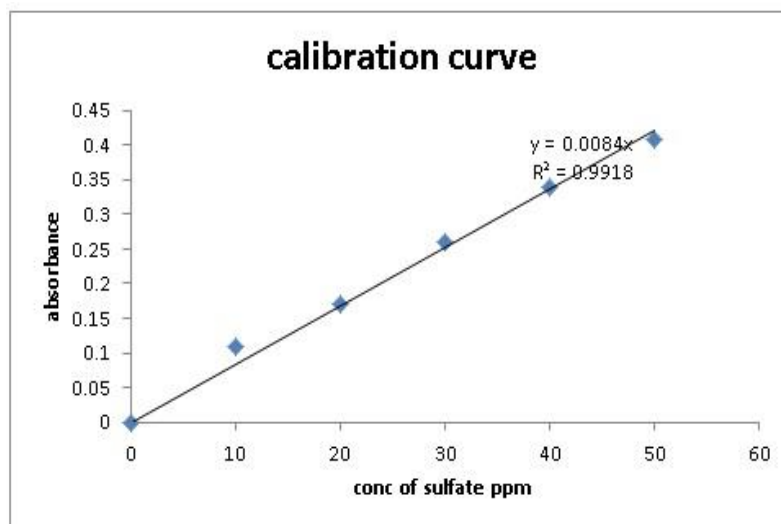


Figure 3.2: Linear calibration curve of absorbance vs. concentration for sulfate.

3.7. Determination of sulfate –ion contamination

The concentration of sulfate –ion concentration in the water sample was measured by transferring certain volume of water sample into a 100ml volumetric flask. Then 2ml of 1M HCL were added, followed by 2ml of 25% barium chloride solution. The volume was completed to the mark with distilled water, stopper and shaken for 1min by inverting several times. The absorbance was measured and the concentration was determined using the constructed calibration curve.

3.8. Batch Experiment

The variables that affect the adsorption behavior of the new surface with sulfate were studied. These variables include the effect of pH, temperature, concentration of sulfate-ion concentration, dose of adsorbent and the contact time. The adsorption capability of the new surface was inspected using kinetics and pH effects. Equilibrium isotherm studies were achieved by changing the following parameters: temperature, initial concentration of sulfate solution and adsorbent dose on sulfate adsorption process from the solution.

3.8.1. Effect of contact time

Adsorption of sulfate on the new surface was intended as a function of time at 20°C. A sample of 50 mL of sulfate (20 mg/L) solution at pH 3.7 was taken in a volumetric flask and shaken with 0.005g of adsorbent. At the end of time interval (10, 20, 30, 40 and 50 minute) every sample was filtrated and the quantity of adsorbed sulfate was specified using UV-spectroscopy.

3.8.2. Effect of temperature

To examine the influence of temperature on adsorption, 0.005 g samples of the new adsorbent were added to 50 mL of sulfate solutions of concentration 20 mg/L at pH 3.7. Every mixture was put in water bath at the required temperature (15 - 55°C) with shaking for 30 min., at the end of time interval, each sample was filtrated and the quantity of adsorbed sulfate was specified by UV-spectroscopy.

3.8.3. Effect of pH

Impact of initial pH on adsorption process was inspected in pH range (2-12). The pH was set by using of 0.1M HCl and 0.1M NaOH. 0.005 g of adsorbent samples was added to 50 mL of 20 mg/L of sulfate solutions. The mixtures were positioned in water bath with shaking at a specific temperature (30°C) for 30 min. After passing the assigned time interval, each sample was filtrated and the quantity of adsorbed sulfate was specified by UV-spectroscopy.

3.8.4. Effect of adsorbent dose

The impact of adsorbent dose on the adsorption process of sulfate was studied. To find out the most favorable adsorbent dose, 0.005, 0.01, 0.015, 0.02 g and 0.025 of the new adsorbent were added to five phials have 50 mL of 20mg/L sulfate solution at pH 2.5 . The mixtures were placed in water bath with shaking at constant temperature (30°C) for 30 min. After passing the assigned time , every sample was filtrated and the quantity of adsorbed sulfate was specified by UV-spectroscopy.

3.8.5. Effect of initial concentration of sulfate

To specify the best concentration of sulfate ion on adsorption process, 0.015 g of adsorbent was added to a group of phials with 50 mL of different concentrations of sulfate solution (10-50 mg/L), under the most effective temperature (30°C) and pH 2 for 30 min. The absorbance of each solution after filtration was measured by UV-spectrophotometer.

Chapter Four

Results and Discussion

4.1. Characterization of Materials

4.1.1. SEM Characterization

The Scanning Electron Micrographs (SEM) was done, at 500 magnifications, on the free silica and chemically modified silica (Si-RO-PzPyr) to reveal variation between the two surfaces. The SEM (Figure 4.1) clarifies the Non-agglomerated silica particles after treatment which supports allegations of the well-organized allocation of the functional group on the entire surface. It was obvious that the packed functional groups were spread on the total surface which made the surface of the new product (Si-RO-PzPyr) be rough [40].

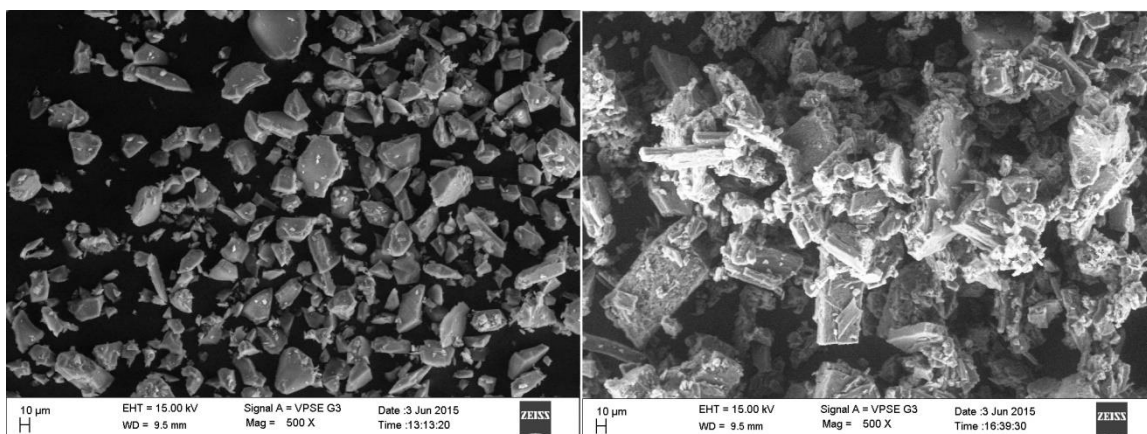


Figure 4.1: SEM micrographs of Free Silica and the synthesized surface (Si-RO-PzPyr).

4.1.2. IR characterization of the material

IR-spectra (Fig. 4.2)[7] of the altered silica demonstrates the intense decrease of the large $\nu(\text{O-H})$ adsorption about 3300 cm^{-1} and the occurrence of $\nu(\text{C-H})$ weak band at $3000\text{-}2800\text{ cm}^{-1}$ conformable to the organic receptor linked to the inorganic matrix. One more distinctive band $\nu(\text{Si-OH})$ which allocated for silanol groups was noticed around 965 cm^{-1} for the activated silica. After immobilization of the organic groups, such band was extremely decreased as anticipated in such processes. In addition to these bands; the modified silica has the characteristic C=N and C=C stretching vibrations at 1637 and 1491 cm^{-1} respectively [7][39][40][43].

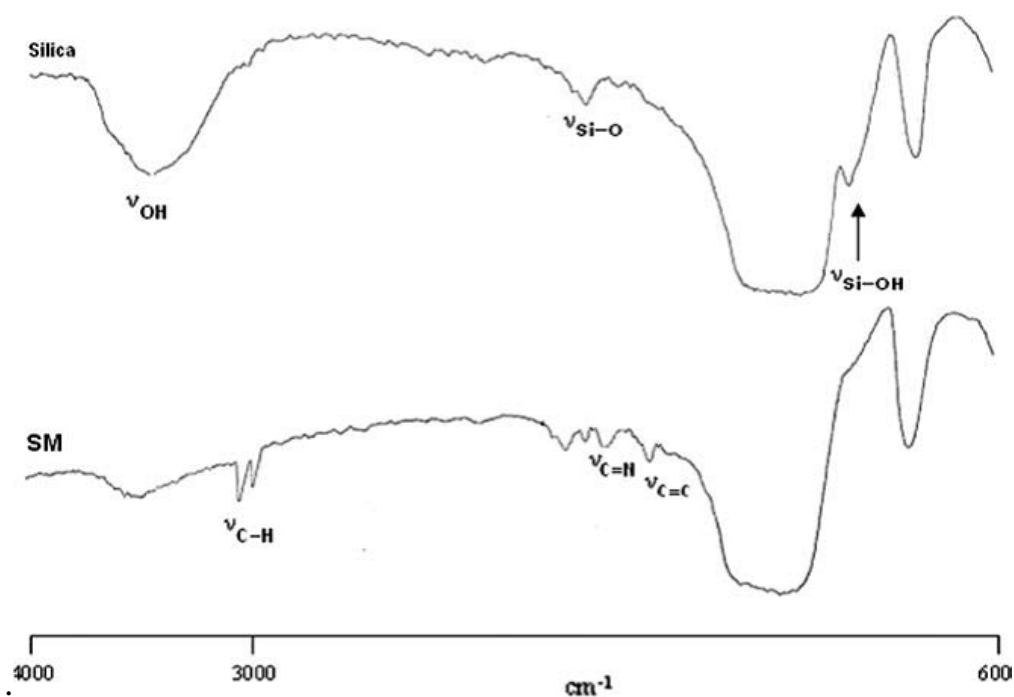


Figure 4.2: IR spectra of pure silica and modified silica.

4.1.3. Thermo gravimetric analysis

The resulting thermogravimetric curve reflect the thermal stability of the modified substance as shown in Figure (4.3) the quantity decomposed in each stage confirms the amount of the compounds grafted. (FS) indicated two losses attributed to physisorbed water molecules released and to condensation of silanol group bonded to the surface .the curve including epoxy groups (Si-Ep) gave a mass loss after the discharge of physically adsorbed water, of 12.84% in the 250–700°C. The target product (MS) exhibited an increase of mass loss due to the decomposition of the organic part immobilized on the surface of silica gel, together with the condensation of the residual silanol groups. The clear increase in mass loss for the mass matrix refers to the large amount of the anchored organic groups [7][43][44].

Figure (4.3) shows the process of degradation between 200-700°C, which emphasizes the high thermal stability for the new product [7].

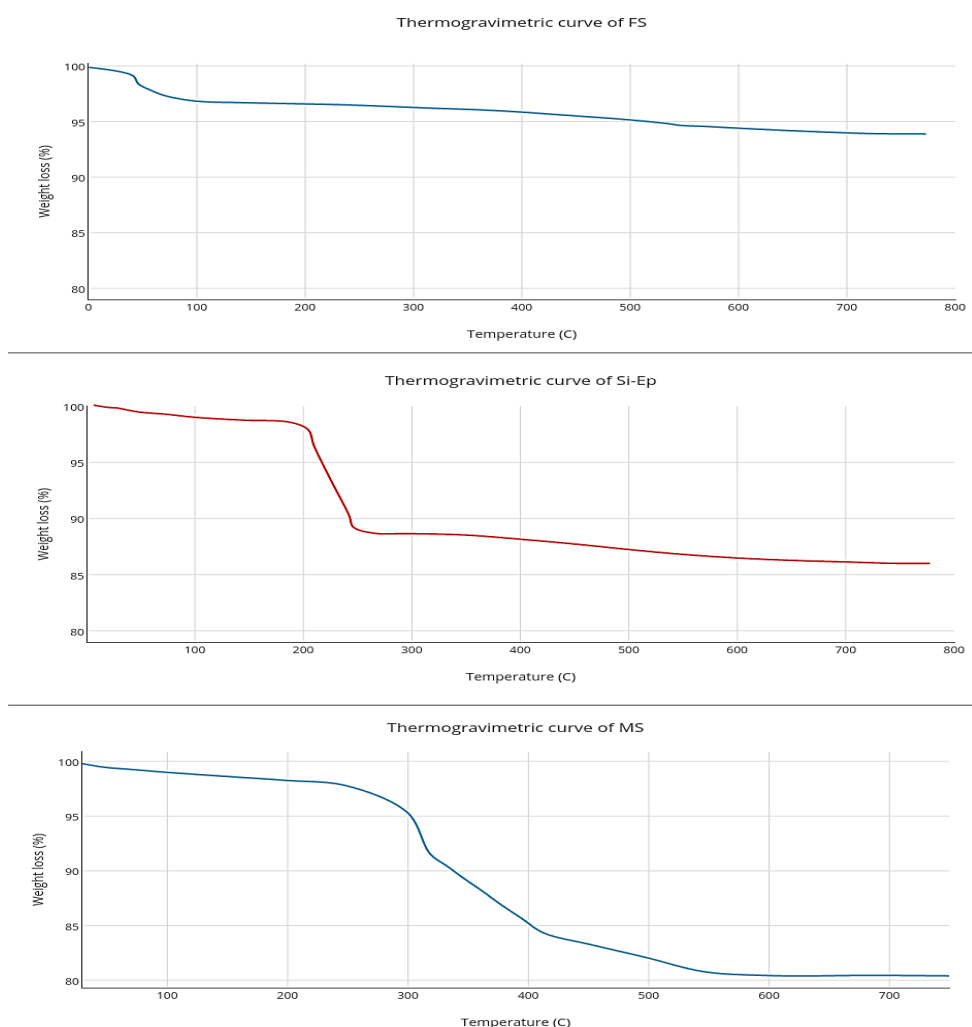


Figure 4.3: Thermogravimetric curves for silica (FS), epoxy silica (Si-Ep) and the new modified surface (MS).

4.2. Investigation of adsorption parameters

4.2.1. Effect of contact time on sulfate adsorption

To determine the optimum contact time for effective removal of sulfate by (Si-RO-PzPyr); the adsorption of sulfate on (Si-RO-PzPyr) was studied as a function of contact time. It can be noticed from Fig. (4.4) the highest percentage removal of sulfate was after 30 min time of shaking.

This percentage removal was 90% and after that it becomes approximately constant.

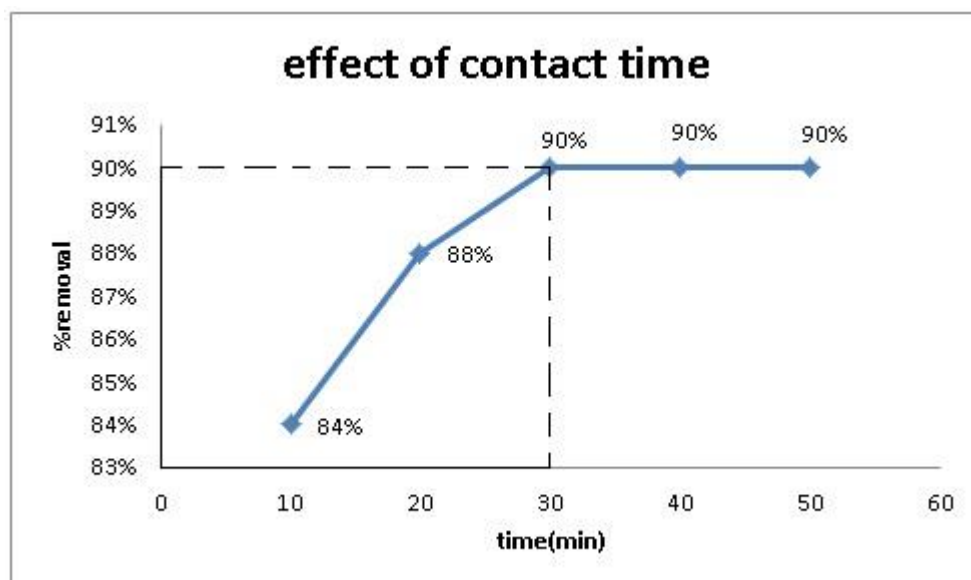


Figure 4.4: effect of contact time to specify the best period of time to achieve a maximum adsorption of sulfate. (Temp.= 25°C, pH= 3.7, conc. of sulfate = 20mg/L, sol. Volume= 50 mL, adsorbent dose= 0.005 g).

The adsorption intake rate is high at first which is due to the great surface area of adsorbent ready for adsorption of sulphate. At the beginning of the adsorption process all reaction positions are unoccupied; therefore the amount of removal is high. After the initial fast adsorption, the rate of adsorption reaches nearly a constant value.

4.2.2. Temperature effect on sulfate adsorption

The effect of temperature on the adsorption rate of sulfate was studied at different temperature from (15-55)°C as shown in Fig. (4.5). It has been noticed that the adsorption of sulfate increased with increasing the

temperature and approaches the maxima at 30°C-35°C. After that the proportion of removal decreases with additional heating, the percentage value of removal at the optimum temperature was 96.8%.

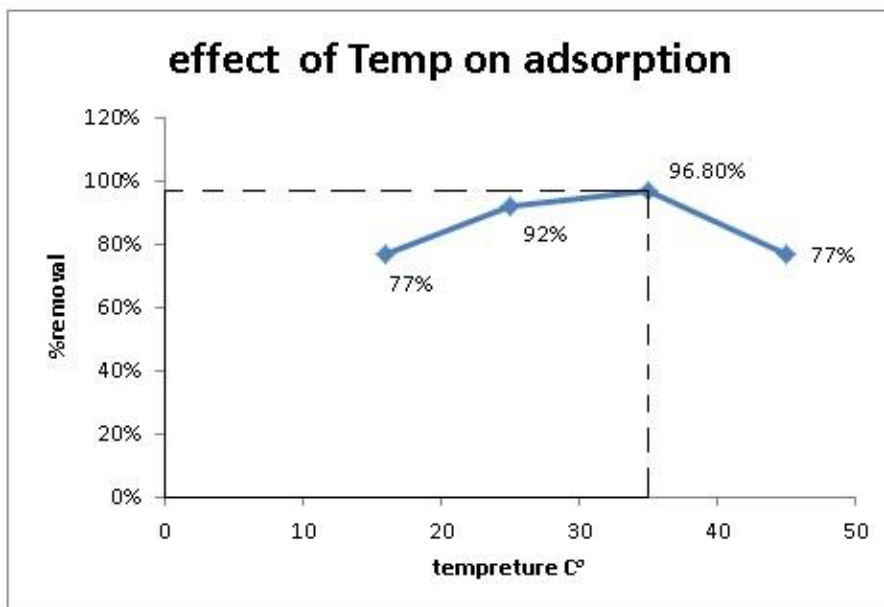


Figure 4.5: effect of temperature on sulfate adsorption. (C_0 = 20 mg/L, time= 20 min., adsorbent dose= 0.005 g, sol. Volume= 50 mL pH=3.7).

4.2.3. Effect of pH on sulfate adsorption

To estimate the effect of pH on the adsorption capability of the modified new surface (Si-RO-PzPyr), experiments were accomplished with solutions of various pH values as shown in the figure (4.6).

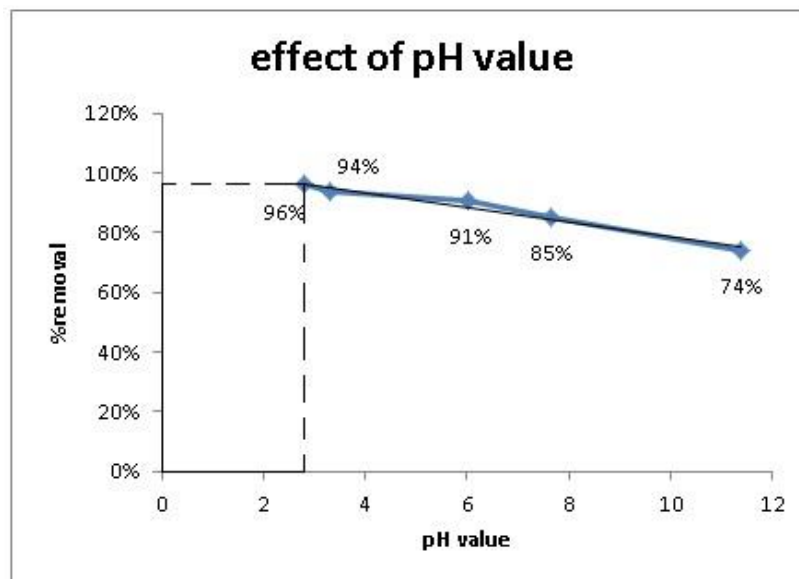


Figure 4.6: pH effect on sulfate adsorption. ($C_0 = 20$ ppm, time= 30 min., $T = 30^\circ\text{C}$, adsorbent dose= 0.005 g, sol. Volume= 50 mL).

The removal of sulfate was at max value at pH 2.0 while this value decreases as pH increases. Protonation degree of surface was high at pH 2.0 thus the surface exhibited maximum positive charge for best adsorption of sulfate. Sulfate anions in acidic solutions are substituted with the counter anions on the protonated amine spots. If the pH of solution is increased, the protonation degree of the surface decreases and accordingly the removal of sulfate decreases.

4.2.4. The Effect of amount of adsorbent

The effect of the dosage of adsorbent on removal of sulfate was studied at initial concentration of sulfate solution of 20mg/L initial volume 50ml at 30°C and at pH =2. It was found that the maximum percentage removal of sulfate is 88% when we use 15mg of adsorbent as shown in figure (4.7).

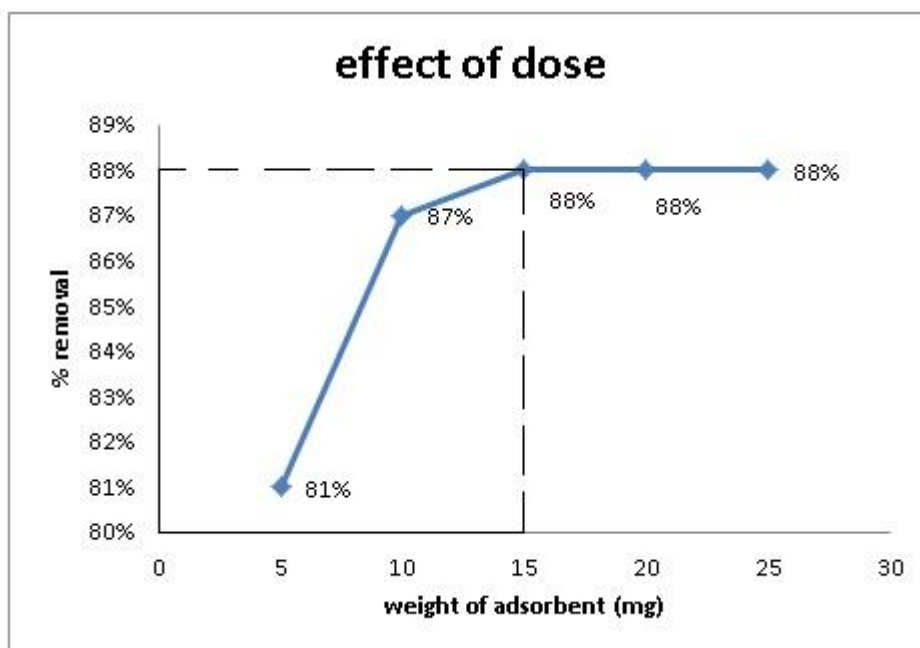


Figure 4.7: The effect of adsorbent dosage on the removal of sulfate. (Temp.= 30°C, time= 20 min., pH= 2, conc. of sulfate= 20 mg/L, sol. Volume= 50 mL).

4.2.5. Effect of sulfate concentration

The influence of the initial concentration of sulfate on the removal activity of the (Si-RO-PzPyr) adsorbent was studied by varying the sulfate concentration while keeping other condition constant as pH, contact time, dosage and temperature. The max percentage of sulfate removal was noticed at lower concentration and as the concentration of sulfate increase the adsorption decrease. Generally, lower initial sulfate concentration has enough adsorption sites available for adsorption process. Maximum percentage removal of sulfate was 85% and then it decreases. Amount of sulfate adsorbed per mass unit of adsorbent increased from 81 to 370 mg/g by increasing sulfate concentration from 10 to 50 ppm. When all condition are considered, the adsorption becomes almost constant whatever

concentration of sulfate is increased. This points formation of a monolayer adsorption on the new modified surface.

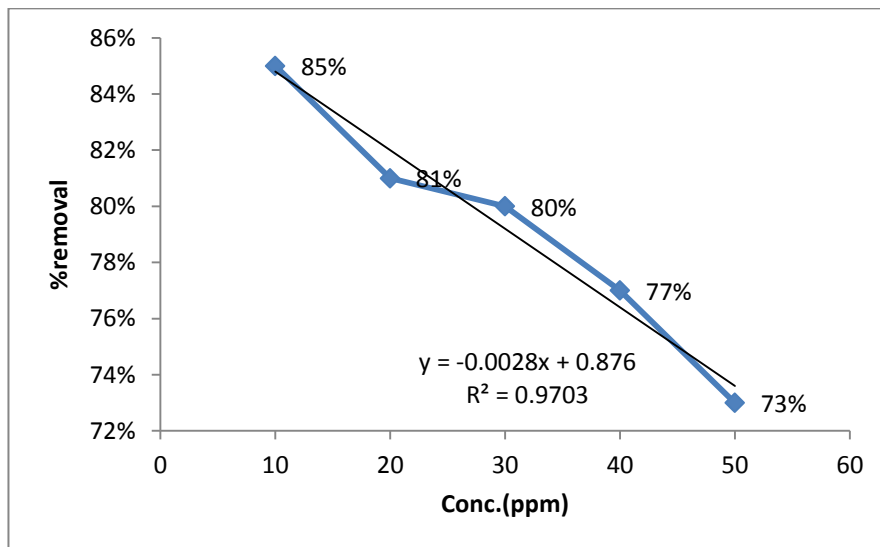


Figure 4.8: effect of sulfate conc. on adsorption capacity (temp.= 30°C,pH = 2, time 20 min., and adsorbent dosage 1mg).

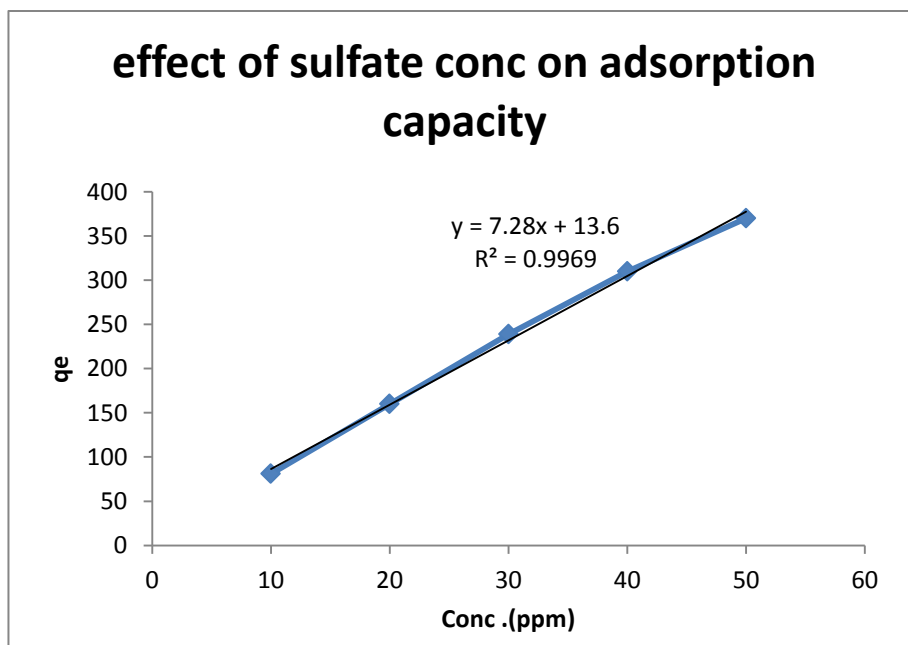


Figure 4.9: effect of sulfate concentration on adsorption capacity (temp30 oC, time 30min, dosage 15 mg).

The partition coefficient (K_d) is a measure of adsorption and is defined as the ratio of the amount of an adsorbate sorbed on a solid to the amount of adsorbate still in solution at equilibrium. The distribution coefficient K_d [44] was calculated from

$$K_d = \frac{\text{amount of sulfate in adsorbent} \times \text{Volume of solution (mL)}}{\text{amount of sulfate in solution} \times \text{mass of adsorbent dose (g)}} \quad (4.1)$$

K_d expression is measured directly in the lab [44]. So

$$K_d = \frac{V_w(C_o - C_e)}{m_{sed} \times C_e} \quad (4.2)$$

Figure (4.10) shows that the distribution ratio (K_d) as a function of concentrations. The K_d values decrease with the increase in sulfate concentration.

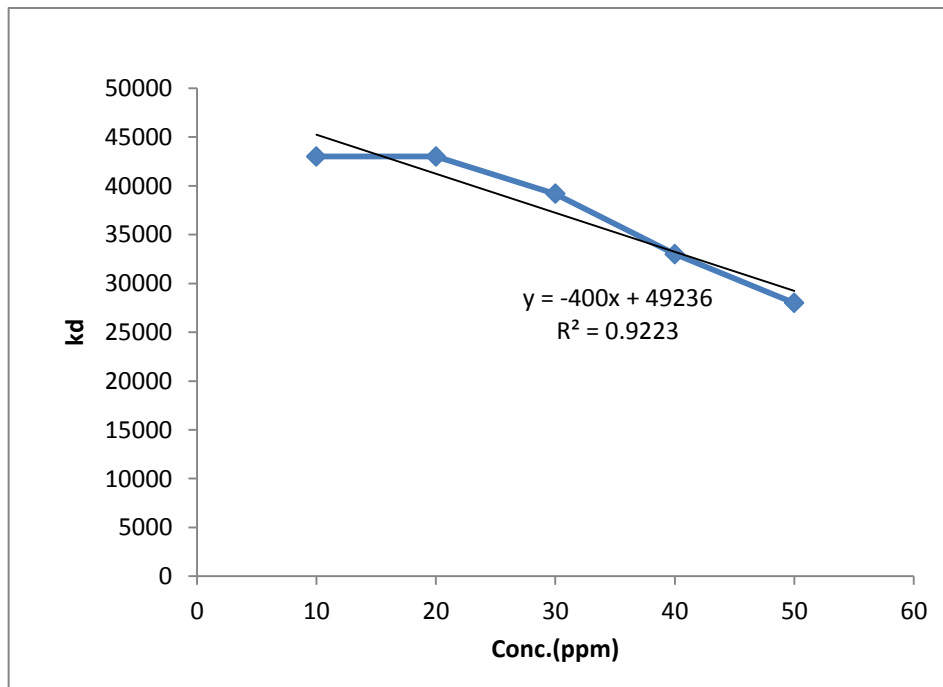


Figure 4.10: effect of sulfate Conc. on the Distribution Ratio (K_d). (Temp.=30°C, time= 30 min., pH= 2, adsorbent dose= 0.015 g, sol. Volume= 50 mL).

Table 4.1: Adsorption parameters

Optimum condition	Time (min)	Temp. (°C)	pH	Weight of adsorbent (g)	Concentration of sulfate (ppm)
	30	30	2.5	0.015g	10ppm
% removal	90%	96.8%	96%	88%	85%

4.3. Adsorption isotherm of sulfate

Studying adsorption equilibrium supplies information about the adsorption capability of the surface. An adsorption isotherm is specified by specific constant values, which clear up the surface characteristics and to compare the abilities of the surface for adsorbing different pollutants. The equilibrium data can be analyzed using known adsorption systems. Different mathematical models can be used to depict the experimental data of adsorption isotherms. Freundlich models, Langmuir and Temkin used for adsorption analysis took place in the experiment.

4.3.1. Langmuir Adsorption Isotherm

This model quantitatively characterizes the formation of a monolayer adsorbate on the outer surface of the adsorbent, and thereafter no adsorption is carried out further. The Langmuir isotherm is good for a monolayer adsorption on a surface has a limited number of similar sites. The model supposes equal adsorption energies on the surface and no migration of adsorbate in the plane of the surface.

Depending on equation (2.1); Q_m and K_L values were calculated from the slope and y- intercept of the Langmuir plot of C_e / Q_e against C_e . Langmuir plots, shown in Figure (4.11) adsorbed amount for formation of monolayer (Q_m), Langmuir constant adsorption-desorption equilibrium (K_L) and the regression constant (R^2) were determined and the values are shown in the table 4.2.

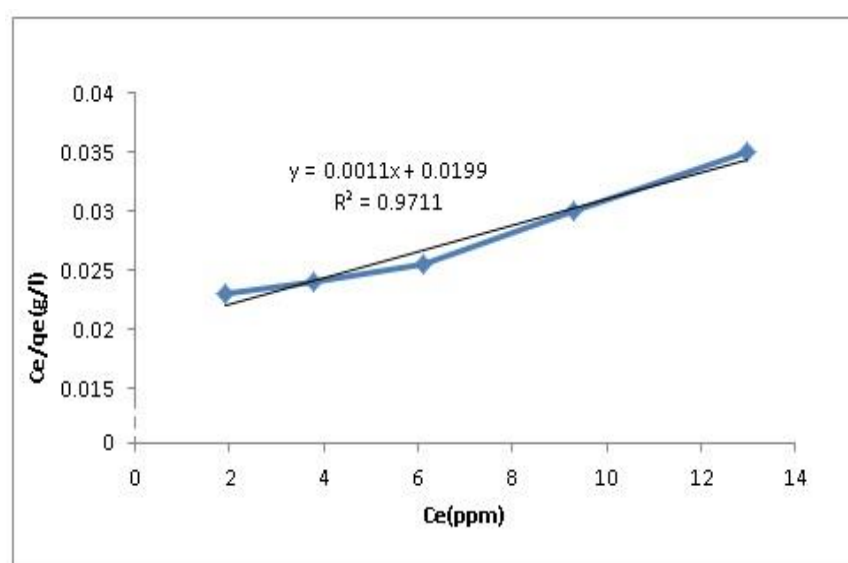


Figure 4.11: Langmuir plot for sulfate adsorption on (Si-RO-PzPyr). (Temp.= 30°C, pH= 2, time= 0 min., sol. Volume= 50 mL, adsorbent dose= 0.01 5g)

Table 4.2: Parameters and correlation coefficient of Langmuir isotherm model for adsorption of sulfate onto (Si-RO-PzPyr)

Langmuir isotherm model parameters				
Adsorbate	Parameters			
	Q_m (mg/g)	K_L (L/mg)	R_L	R^2
(Si-RO-PzPyr)	909	0.055	0.083	0.9711

The R_L value in this study was calculated using equation (2.2). It has been found equal to 0.083 at 35 °C which is between 0 and 1, indicating that the adsorption of sulfate on (Si-RO-PzPyr) is convenient.

4.3.2. Freundlich Adsorption Isotherm

This is usually used to characterize the adsorption features for the heterogeneous surface. The constants K_F and n were determined by using a graph of $\ln(Q_e)$ vs. $\ln(C_e)$, which are $\log K_F$ as Y-intercept and $(1/n)$ as a slope as shown in Figure (4.12)

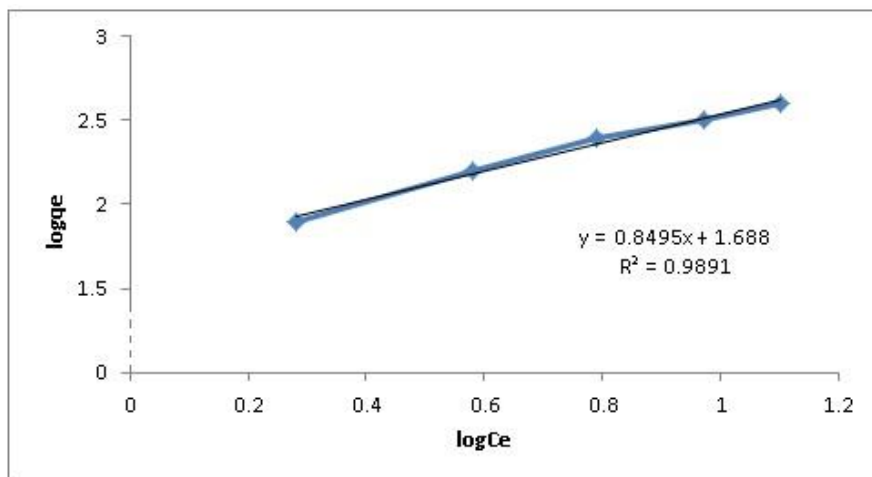


Figure 4.12: Freundlich plot for sulfate adsorption on (Si-RO-PzPyr) (Temp= 30oC, pH= 2, time= 20min., sol. Volume= 50 mL, adsorbent dose= 0.01 g).

Table 4.3: Freundlich Parameters and correlation coefficient for sulfate adsorption on (Si-RO-PzPyr) (Temp= 35°C, pH= 2, time=20min., sol. Volume= 50 mL, adsorbent dose= 0.01 g)

Freundlich isotherm model parameters				
Adsorbate	Parameters			
	1/n	n	$K_F = (\text{mg/g} \cdot (\text{L/mg})^{1/n})$	R^2
(Si-RO-PzPyr)	0.849	1.2	49	0.9891

The data in Table (4.3) presents; the value of $1/n = 0.849$ while $n=1.2$ showing that the adsorption of sulfate on (Si-RO-PzPyr) is convenient and the R^2 value is 0.9891.

4.3.3. Temkin Adsorption Isotherm

Depending on equation (2.5) a plot of Q_e vs. $(\ln C_e)$ can be plotted as shown in Figure (4.13). The constants A, B and b were calculated. All parameters and correlation coefficient are listed in Table (4.4).

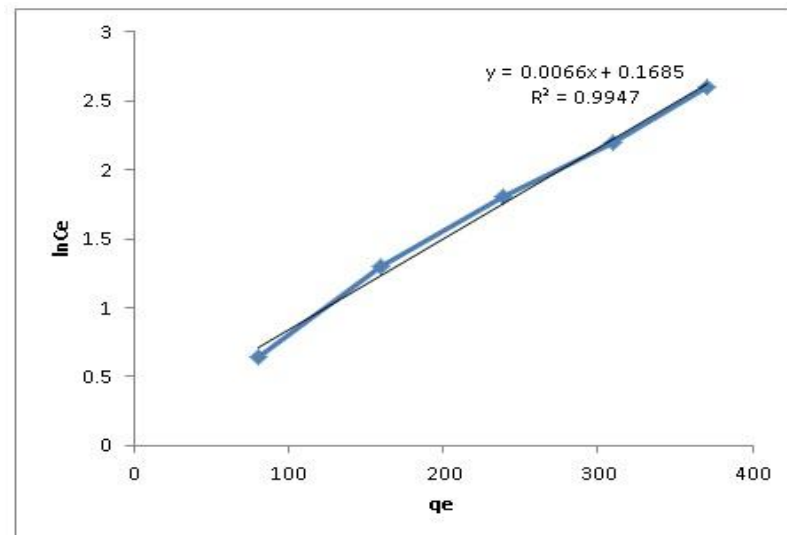


Figure 4.13: Temkin plot for sulfate adsorption on (Si-RO-PzPyr). (Temp.= 30°C, pH=2, time= 40 min., sol. Volume= 50 mL, adsorbent dose= 0.015g).

Table 4.4: Temkin isotherm parameters and correlation coefficient for adsorption of sulfate on (Si-RO-PzPyr)

Temkin isotherm model parameters				
Adsorbate	Parameters			
	A (L/g)	b (J/mol)	B	R²
(Si-RO-PzPyr)	1.2×10^{11}	3.88×10^5	0.0066	0.9947

Three adsorption isotherm models were tested. The adsorption data assigned to Langmuir, Freundlich and Temkin. Using Langmuir isotherm data in Table 4.2, the R_L value in this study was found to be 0.083 at 35 °C pointing that the adsorption of sulfate on (Si-RO-PzPyr) is favorable and the R^2 value is 0.971. From Freundlich isotherm data in the table (4.3), the value of $1/n = 0.849$ while $n = 1.2$ indicating that sulphate adsorption on (Si-RO-PzPyr) is convenient and value $R^2 = 0.9891$. Adsorption of sulfate by (Si-RO-PzPyr) was explained well by Temkin model. Temkin adsorption model has the highest value of regression (0.9947) and thus the best fit.

4.4. Adsorption Thermodynamics

From the Van't Hoff plot (Figure 4.14) ΔH and ΔS can be determined,

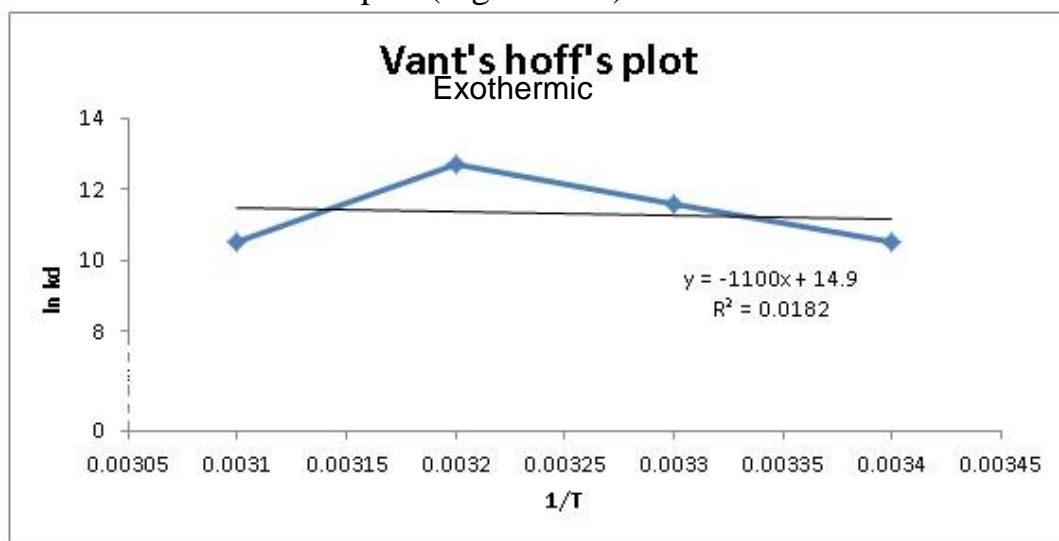


Figure 4.14: A plot of $\ln K_d$ vs. $1/T$ for sulfate adsorption on (Si-RO-PzPyr). (Temp = 35°C, pH= 2, adsorbent dose= 0.005 g, time= 20 min, sol. Volume= 50 mL).

ΔH° and ΔS° were calculated from the slope and y-intercept of a linear plot for $\ln K_d$ against $1/T$. The results display that enthalpy of adsorption ΔH° was 9.1454 kJ mol⁻¹ and ΔS° was 123.88 J mol⁻¹ K⁻¹. ΔG° was studied at various temperatures. Depending on equation (2.7) the thermodynamic values are computed and listed in Table (4.5):

Table 4.5: The thermodynamic values of sulfate adsorption at different temperatures

Adsorbent	ΔH° (KJ/mol)	ΔS° (J/mol.K)	ΔG° (KJ/mol)			
			289 K	298 K	308 K	318 K
(Si-RO-PzPyr)	9.145	123.88	-26.7	-27.8	-29.1	-30.3

According to the results in Table (4.4) table the adsorption of sulfate on (Si-RO-PzPyr) adsorbent is spontaneous ($\Delta S^\circ > 0$) and ($\Delta G^\circ < 0$).

4.5. Adsorption kinetics of sulfate

Kinetic models have been used to examine the mechanism of adsorption and potential rate controlling steps, which is useful for choosing the preferable conditions for full scale process. Pseudo-first-order and pseudo-second-order kinetic models were applied.

Adsorption rate constant k_1 for the sulfate adsorption onto (Si-RO-PzPyr) was specified depending on the straight-line graph of $\log (q_e - q_t)$ vs. t . Data were fitted with a poor correlation coefficient (Table. 4), referring that the rate of removal of sulfate onto (Si-RO-PzPyr) does not conform the pseudo-first-order equation.

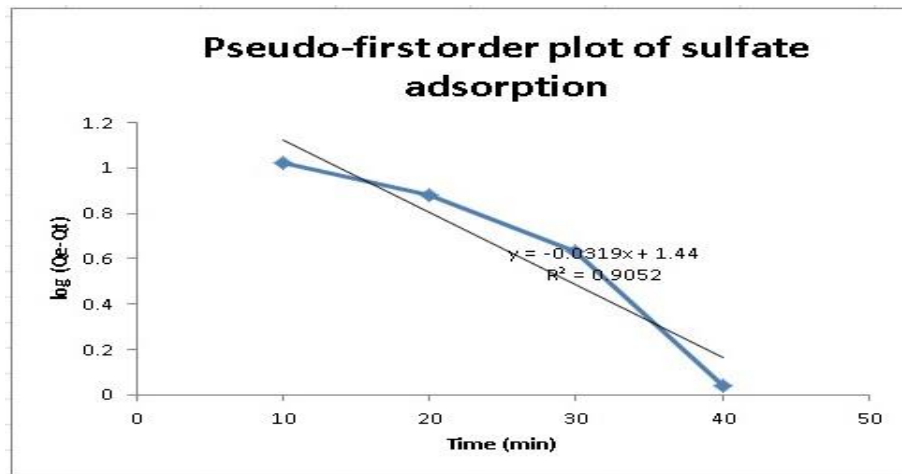


Figure 4.15: Pseudo-first order plot of sulfate adsorption.

Table 4.6: Pseudo first order model rate constants

Q_{exp}	Q_{calc}	R^2	K_1
179	28	0.9052	0.073

K_2 and h values were specified from the slope and the y-intercept of the plots of t/q vs. t as in Figure (4.16). The parameters and correlation coefficient values are presented in Table (4.7). The correlation coefficient of examined data was very high ($R^2 > 0.9981$). This proves that the adsorption of sulfate on (Si-RO-PzPyr) complied with the pseudo-second-order kinetic model. A good approval with this adsorption model was proven by nearly the similar value of calculated Q_e and the experimental one.

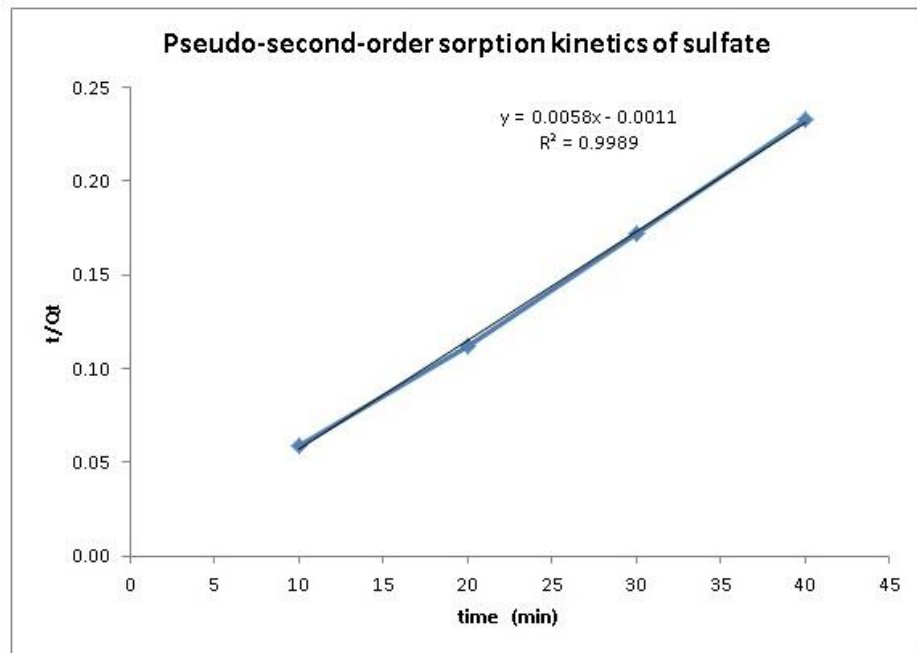


Figure 4.16: Pseudo second order adsorption kinetics of sulfate.

Table 4.7: Pseudo second order parameters for sulfate adsorption

$Q_{e(\text{exp})}$ (mg/g)	$Q_{e(\text{calc})}$ (mg/g)	R^2	K_2 (g/mg min)
172	200	0.9989	0.030

Conclusions

In this study, it is found that the new modified polysiloxane polymer has very good thermal and chemical stabilities, and so it can be used as a good adsorbent to grab sulfate from groundwater. The observed results of this study involve the following:

1. (Si-RO-PzPyr) was able to remove sulfate within the first 30 minutes with high removal efficiency at pH around 2, 30°C Temperature, 0.015g weigh of dose and initial concentration 10 mg/L.
2. Adsorption of sulfate by (Si-RO-PzPyr) was explained well by Temkin model. Temkin adsorption model has the highest value of regression (0.9947) and thus the best fit.
3. The adsorption mechanism conformed with pseudo second-order kinetic adsorption model with correlation coefficient of about one.
4. The thermodynamic parameter of adsorption of sulfate on (Si-RO-PzPyr) is endothermic ($\Delta H > 0$) and spontaneous ($\Delta S > 0$).

Recommendations:

1. Determining the concentration of sulfate in waste water and using this polymer for removing it by adsorption.
2. Test this polymer in removing other pollutants.
3. Removing sulfate by other surface and compare between the adsorption efficiency of them and the synthesized polymer in this research.

References

- [1] Lenntech B.V., Sulfates, **WATER TREATMENT**; 1998-2016; Available from: <http://www.lenntech.com/sulfates.htm>.
- [2] Oram B., **Hydrogen Sulfide, Sulfate Reducing Bacteria - How to Identify and Manage Sulfate**, Water Research Centre, 2014, Available from: <http://www.water-research.net/index.php/sulfates>.
- [3] SaskH2O, **Water Committee, Sulfates**, Government of Saskatchewan - September 25, 2013, Available from:
<http://www.saskh2o.ca/PDF-WaterCommittee/sulphate.pdf>.
- [4] Salman M. S., Sep. 2009, **Removal of Sulfate from Waste Water by Activated Carbon**, Vol. 5, No. 3, p 72 – 76.
- [5] Thomas W.J., Crittenden B.D., **Adsorption technology and design**, Oxford, UK, Elsevier Science & Technology Books, 1998, 289 p.
- [6] Radi S., Toubi Y., Attayibat A., Bacquet M., 2011, *New Polysiloxane-Chemically Immobilized C,C-Bipyrazolic Receptor for Heavy Metals Adsorption*, Journal of Applied Polymer Science, Vol. 121: 1393–1399.
- [7] Radi S., Attayibat A., Ramadani A., Bacquet M., 2010, *Synthesis and Characterization of Novel Porous SiO₂ Material Functionalized with C,C-Pyridylpyrazole Receptor*, Journal of Applied Science, Vol. 117: 3345–3349.

[8] UNEP, (2003), **Desk study on the Environment in the Occupied Palestinian Territories**, 188 p.

[9] Anayah F., Almasri M., 2009, **Trends and occurrences of nitrate in the groundwater of the West Bank- Palestine**, Applied Geography, 29: 588–601.

[10] Anayah F., 2006, **An Assessment of the Nitrate and Chloride in the West Bank Groundwater Resources using GIS**, MSc Thesis, Nablus-Palestine, An-Najah National University.

[11] U.S. Geological Survey, Jan. 2014, **What is Ground Water, Water Resources Division**, Open File Report 93-643, available from:

<http://pubs.usgs.gov/of/1993/ofr93-643/>.

[12] Environment and Climate Change Canada, Aug. 2010, **Groundwater Contamination**, Available from:

<https://www.ec.gc.ca/eau-water/default.asp?lang=En&n=6A7FB7B2-1>.

[13] US EPA Seminar Publication, **Ground Water Contamination, A Guide for Small Communities**, Chapter 3 Available from:

<https://www.epa.gov/sites/production/files/2015-08/documents/mgwc-gwc1.pdf>.

[14] Lougue Keith, Corwin Dennis L., 2005, **Point and NonPoint Source Pollution, Encyclopedia of Hydrological Sciences**, John Wiley & Sons. Available from:

<https://www.researchgate.net/publication/227986732>.

[15] World Health Organization, 2004, **Sulfate in Drinking-water**, 3rd Ed. Available from:

http://www.who.int/water_sanitation_health/dwq/chemicals/sulfate.pdf.

[16] J. B. Calvert, Jan. 2003, **Sulphur**, Available from:

<http://mysite.du.edu/~jcalvert/phys/sulphur.htm>.

[17] Smith R.L., **Ecology and field biology**, (1974), 2nd edition. Harper & Row, New York, NY.

[18] Barry G.S., **Sodium sulphate**, In: Canadian minerals yearbook, 1988, Mineral Report No. 37, Mineral Resources Branch, Energy, Mines and Resources Canada, Ottawa (1989).

[19] Patil S. Z., Unnithan A.R., Unnikrishnan G., June 2014, Biosulphidogenesis: *Isolation and characterization of Thermodesulfobacterium commune sp. nov. Isolated from hot water springs of Thane, Maharashtra.*, Journal of Pharmacy and Biological Sciences, Volume 9, Issue 3 Ver. III (May -Jun. 2014), PP 09-13.

[20] Delisle, C.E., Schmidt, J.W., **The effects of sulphur on water and aquatic life in Canada**, In: Sulphur and its inorganic derivatives in the Canadian environment, NRCC No. 15015, Associate Committee on Scientific Criteria for Environmental Quality, National Research Council of Canada, Ottawa.

[21] McKee, J.E., Wolf, H.W., **Water quality criteria**, 1963, 2nd edition, California State Water Quality Control Board, Sacramento, CA (1963).

[22] KELLER W., PITBLADO J. R., Feb. 1986, **Water quality changes in Sudbury area lakes**: A comparison of synoptic surveys in 1974–1976 and 1981–1983, *Water, Air, and Soil Pollution*, 29 (1986): 285-296.

[23] XAmplified: **Free Education Online Resource**, Adsorption, 2010, Available at: <http://www.chemistrylearning.com/adsorption/>.

[24] Piccin J., Dotto G., Pinto L. 2011 April/ June, *Adsorption Isotherms and Thermochemical Data of FD&C RED N° 40 Binding by Chitosan*, *Brazilian Journal of Chemical Engineering*, Vol. 28 (2): 295 – 304.

[25] Rahimi M, Vadi M., 2014 May 19, *Langmuir, Freundlich and Temkin Adsorption Isotherms of Propranolol on Multi-Wall Carbon Nanotube*, *Journal of Modern Drug Discovery and Drug Delivery Research*; 1-3.

[26] Foo K., Hameed B., 2009 Sep. 7, **Insights into the modeling of adsorption isotherm systems**, *Chemical Engineering J.*, 156: 2–10.

- [27] Dada A., Olalekan A., Olatunya A., DADA O., 2012 Nov. – Dec, Langmuir, Freundlich, Temkin and Dubinin – *Radushkevich Isotherms Studies of Equilibrium Sorption of Zn²⁺ Unto Phosphoric Acid Modified Rice Husk*, IOSR Journal of Applied Chemistry, Vol. 3 (1): 38-45.
- [28] Joseph J., Xavier N., 2013, **Equilibrium and kinetic studies of Methylene blue onto activated carbon prepared from Crescentiacujete fruit shell**, Nature and Science J; 11 (4): 53-58.
- [29] Kamal H., 2014, *Removal of Methylene Blue from aqueous solutions using composite hydrogel prepared by gamma irradiation*, Journal of American Science; 10 (4): 125-133.
- [30] Chen X., 2015 January 22, **Modeling of Experimental Adsorption Isotherm Data**, Information, 6: 14-22.
- [31] Gueu S., B. Yao, K. Adouby, G. Ado, **Kinetics and thermodynamics study of lead adsorption on to activated carbons from coconut and seed hull of the palm tree**, Dec. 2007, Int. J. Environ. Sci. Tech., 4 (1): 11-17.
- [32] Abramian L., El-Rassy H., 2009, *Adsorption kinetics and thermodynamics of azo-dye Orange II onto highly porous titania aerogel*, Chemical Engineering Journal; 150: 403–410.
- [33] Martins A. E., Pereira M. S., Jorgetto A. O., Martines M. A.U., Silva R. I.V., Saeki M. J., Castro G. R., Feb. 2013, **The reactive surface of Castor leaf [*Ricinus communis* L.] powder as a green adsorbent for the**

removal of heavy metals from natural river water, Applied Surface Science 276 (2013) 24–30.

[34] YUH-SHAN HO, **Citation review of Lagergren kinetic rate equation on adsorption reactions**, Oct. 2003, Vol. 59, No. 1 (2004) 171-177.

[35] Hashem A., El-Khiraigy K., **Bioadsorption of Pb(II) onto Anethumgraveolens from Contaminated Wastewater: Equilibrium and Kinetic Studies**, Dec. 2012, Journal of Environmental Protection, 2013, 4, 108-119.

[36] Corrosionpedia, **Polysiloxanes**, Available at:

<https://www.corrosionpedia.com/definition/1842/polysiloxanes>.

[37] N. M. El-Ashgar and S. M. Saadeh, 2006, **Preparation of Immobilized Polysiloxane Salicylaldehyde Propylimine and Its Application**, J. Al-Aqsa Univ., 10, 153-161.

[38] I.M El-Nahhal, N.M. El-Ashgar, M.M. Chehimi, P. Bargiela, J. Maquet, F. Babonneau and J. Livage, 2003, **Metal uptake by porous iminobis (N-2-aminoethylacetamide)-modified polysiloxane ligand system**, Microp. Mesop. Mat., 65(2-3), 299-310.

[39] Radi S., Tighadouini S., Toubi Y., Bacquet M., 2010 Sep. 7, ***Polysiloxane surface modified with bipyrazolic tripodal receptor for***

quantitative lead adsorption, Journal of Hazardous Materials, 185: 494–501.

[40] Radi S., Tighadouini S., Bacquet M., Degoutin S., Cazier F., Zaghrioui M., Mabkhot Y., 2014, **Organically Modified Silica with Pyrazole-3-carbaldehyde as a New Sorbent for Solid-Liquid Extraction of Heavy Metals**, Molecules; 19: 247-262.

[41] **Sigma-Aldrich, Product Specification**, product number: 24857354, USA available from: www.sigmaaldrich.com.

[42]Sigma-Aldrich, Product Specification, product number: 24867573, USA available from: www.sigmaaldrich.com.

[43] Radi S., 2,Basbas N., Tighadouni S., Bacquet M., Degoutin S., Cazier F., New Amine-Modified Silicas: Synthesis, Oct. 2013, **Characterization and Its Use in the Cu(II)-Removal from Aqueous Solutions**, Progress in Nanotechnology and Nanomaterials, Vol. 2 Iss. 4, PP. 108-116.

[44] Jodeh Sh., Amarah J., Radi S., Hamed O., Warad I., Salghi R., Chetouni A., Samhan S., Alkoni R., Jan 2016, **Removal of methylene blue from industrial wastewater in Palestine using polysiloxane surface modified with bipyrazolic tripodal receptor**, Mor. J. Chem. 4 N°1 (2016)140-156.

[45] Oliver J. Hao , Jin M. Chen , Li Huang & Robert L. Buglass, Sulfate- reducing bacteria, *Critical Reviews In Environmental Science And Technology*, Vol. 26 , Iss. 2,1996, Pages 155-187, Available from:

<http://www.tandfonline.com/doi/abs/10.1080/10643389609388489?journalCode=best20>.

[46] Isaac, Jad, **The role of groundwater in the water conflict and resolution between Israelis and Palestinians**, Applied Research Institute- Jerusalem, Available from: www.arij.org.

[47] Mediterranean Environmental Technical Assistance Program,

Water Quality Management, Available from:

<http://siteresources.worldbank.org/EXTMETAP/Resources/WQM-WestBankGazaP.pdf>.

[48] Assessment of Groundwater Quality in the Gaza Strip, **Palestine Using GIS Mapping**, Shomar B., Abu Fakher S.,Yahya A., J. Water Resource and Protection, 2010, 2, 93-104.

جامعة النجاح الوطنية

كلية الدراسات العليا

توليف وتوصيف مادة مسامية جديدة من السيليكا المعدلة بمستقبلات (كربون،
كربون - بايريديل بايرازول) لإزالة الكبريتات من مياه الصرف الصحي

إعداد

دينا عدنان علي خضرية

إشراف

أ.د. شحدة جودة

أ.د. اسماعيل ورّاد

قُدّمت هذه الأطروحة استكمالاً لمتطلبات الحصول على درجة الماجستير في الكيمياء من كلية
الدراسات العليا في جامعة النجاح الوطنية، نابلس - فلسطين

2016

ب

توليف وتوصيف مادة مسامية جديدة من السيليكا المعدلة بمستقبلات (كربون, كربون بايريديلبايرازول) لإزالة الكبريتات من مياه الصرف الصحي

إعداد

دينا عدنان علي خضرية

إشراف

أ.د. شحدة جودة

أ.د. اسماعيل وزاد

الملخص

تتسرب الملوثات المختلفة يوميا إلى المياه الجوفية والتي تشكل المصدر الأساسي للمياه في فلسطين. أحد هذه الملوثات هي الكبريتات, التراكيز العالية من الكبريتات يمكنها أن تحدث خلا في دورة الكبريتات في الطبيعة مما يتسبب في مشاكل صحية لكل من الانسان والحيوان.

يشمل هذا البحث على تعديل سطح السيليكا (silica gel) المسامية النقية بإضافة 3-glycidoxypropyltrimethoxysilane إلى سطح السيليكا ومن ثم ربط C,C-pyridylpyrazole إلى هذه التفرعات , حيث تفتح حلقة الإيبوكسيد لتشكل مجموعة من المستقبلات مما يزيد من قدرة السطح المعدل على الامتزاز.

في هذا البحث تم تعديل سطح السيليكا وتشخيص طبيعة السطح المعدل وتوصيفهم خلال تحليل العناصر ومطياف الأشعة تحت الحمراء (IR) ومجهر المسح الإلكتروني (SEM), حيث أظهرت صور المسح الإلكتروني (SEM) أن السطح المعدل الجديد يتميز بخصائص تجعله قادرا على الامتزاز, كما تم اختبار الاستقرار الحراري للمادة الجديدة باستخدام (Thermogravimetry), وقد أظهرت نتائج الاختبارات استقرارا وثباتا حراريا يمكن الاستدلال عليه من خلال دراسة منحنيات التحليل الحراري لها.

للتعرف على مدى قدرة المادة الجديدة على امتزاز الكبريتات من المحلول, تم قياس تركيز الكبريتات في السائل قبل اضافة المادة المازة وقياس تركيز الكبريتات بعد إضافتها وإعطاءها المدة

ج

المحددة للاتصال, وذلك باستخدام مطياف الأشعة فوق البنفسجية (UV-Spectrophotometry). ومن أجل التحقق من كفاءة المادة الجديدة على امتزاز الكبريتات وتحديد الظروف المثلى لذلك, تم دراسة العوامل والظروف المختلفة وتأثيرها على كفاءة السطح الجديد المعدل على امتزاز الكبريتات. وقد أجريت تجارب عديدة تحت ظروف ومتغيرات مختلفة مثل: درجة الحرارة, درجة الحموضة, تركيز الكبريتات, كمية المادة المازة ومدة الاتصال. وقد لوحظ من خلال هذه التجارب أن نسبة إزالة الكبريتات من المحاليل المائية قد ازدادت مع زيادة كمية المادة المازة ومدة الاتصال وازدادت قليلا بزيادة درجة الحرارة لغاية 35 درجة مئوية, كمية المادة المازة ومدة الاتصال, بينما انخفضت هذه النسبة بزيادة تركيز الكبريتات وزيادة درجة الحموضة.

كما أن عملية الامتزاز هذه ووفقا لقيمة معامل الارتباط يمكن وصفها وفقا لنموذج Temkin, كما أظهرت نتائج البحث بأن آلية الامتزاز هذه يمكن تصنيفها وفقا للنماذج الآلية الحركية للتفاعلات ضمن التفاعلات من الدرجة الثانية (pseudo-second-order). بالإضافة لذلك تبين لنا من خلال دراسة رسم (Van't Hoff) لهذا الامتزاز بأن عملية الامتزاز ماص للحرارة حيث $(\Delta H^\circ > 0)$ وتلقائية حيث $(\Delta S^\circ > 0)$. وعليه يمكن اعتبار (Si-RO-PzPyr) مادة فعالة في إزالة الكبريتات من مياه الصرف الصحي.